

Semileptonic charm decays $D \rightarrow \pi \ell \nu_\ell$ and $D \rightarrow K \ell \nu_\ell$ from QCD Light-Cone Sum Rules

A. Khodjamirian ^(a), Ch. Klein ^(a), Th. Mannel ^(a) and N. Offen ^(b)

^(a) *Theoretische Physik 1, Fachbereich Physik, Universität Siegen,
D-57068 Siegen, Germany*

^(b) *Laboratoire de Physique Theorique CNRS/Univ. Paris-Sud 11,
F-91405 Orsay, France*

We present a new calculation of the $D \rightarrow \pi$ and $D \rightarrow K$ form factors from QCD light-cone sum rules. The \overline{MS} scheme for the c -quark mass is used and the input parameters are updated. The results are $f_{D\pi}^+(0) = 0.67_{-0.07}^{+0.10}$, $f_{DK}^+(0) = 0.75_{-0.08}^{+0.11}$ and $f_{D\pi}^+(0)/f_{DK}^+(0) = 0.88 \pm 0.05$. Combining the calculated form factors with the latest CLEO data, we obtain $|V_{cd}| = 0.225 \pm 0.005 \pm 0.003$ $_{-0.012}^{+0.016}$ and $|V_{cd}|/|V_{cs}| = 0.236 \pm 0.006 \pm 0.003 \pm 0.013$ where the first and second errors are of experimental origin and the third error is due to the estimated uncertainties of our calculation. We also evaluate the form factors $f_{D\pi}^-$ and f_{DK}^- and predict the slope parameters at $q^2 = 0$. Furthermore, calculating the form factors from the sum rules at $q^2 < 0$, we fit them to various parameterizations. After analytic continuation, the shape of the $D \rightarrow \pi, K$ form factors in the whole semileptonic region is reproduced, in a good agreement with experiment.

1. Introduction

Recent measurements of the semileptonic $D \rightarrow \pi \ell \nu_\ell$ and $D \rightarrow K \ell \nu_\ell$ decays by CLEO collaboration [1, 2] provide new accurate results on branching fractions and differential decay rates, in addition to the previously accumulated data [3, 4, 5, 6]. The decay rate distributions in the bins of the variable q^2 (the invariant mass squared of the lepton pair), yield the products of transition form factors and CKM matrix elements, $|V_{cd}|f_{D\pi}^+(q^2)$ and $|V_{cs}|f_{DK}^+(q^2)$. In addition, the form factor shapes are reconstructed and fitted to various parameterizations. With the new data available, it is timely to update the theoretical analysis of the $D \rightarrow \pi$ and $D \rightarrow K$ form factors, aiming at more accurate determination of $|V_{cd}|$ and $|V_{cs}|$.

In this paper, we recalculate the $D \rightarrow \pi, K$ form factors from QCD light-cone sum rules (LCSR's). In this method [7], the correlation function of quark currents is constructed in a form of a transition matrix element between the vacuum and the final hadron state. In our case, the quark current with D -meson quantum numbers is correlated with the charmed weak current, whereas the hadron state is the on-shell pion or kaon. Two different representations of the correlation function are then equated: the operator-product expansion (OPE) near the light-cone and the dispersion integral over hadronic states. In the latter, the ground D -meson contribution containing the $D \rightarrow \pi$ or $D \rightarrow K$ form factor is singled out. Applying the quark-hadron duality approximation, the remaining dispersion integral over the higher states is replaced by the integral over the OPE spectral density. The LCSR approach, though having a limited accuracy, provides analytical expressions for the form factors, in terms of finite quark masses and universal light-cone distribution amplitudes (DA's) of pion or kaon. Importantly, the heavy-light form factors calculated from LCSR's with gluon radiative corrections, include both "hard-scattering" and "soft-overlap" components, and the latter is predicted to be the dominant one.

The fact that the correlation function is calculated at a finite heavy quark mass, simplifies our task, because the OPE of b -quark and c -quark currents have the same analytical expressions. Only the quark mass value has to be changed and the normalization scales have to be adjusted. Hence, for example, the LCSR for $f_{D\pi}^+$ represents a by-product of the LCSR obtained for $f_{B\pi}^+$. The latter form factor used to determine $|V_{ub}|$ is the most familiar application [8, 9, 10, 11, 12, 13] of this method¹. In what follows, we employ the recent update of LCSR for $B \rightarrow \pi$ form factors presented in [13]. Importantly, the $D \rightarrow \pi, K$ form factors obtained from the sum rules, being confronted with experimental data, provide an important test of the whole method.

Compared with the previous calculations of $D \rightarrow \pi, K$ form factors from LCSR's [15, 16], certain modifications and improvements are made. First of all, following [13], we systematically use the \overline{MS} scheme for the c -quark mass, whereas earlier calculations switched to the pole mass in the final sum rules. In this respect we benefit from recent accurate determinations [17] of the c -quark mass from the charmonium QCD sum rules.

¹Interestingly, one of the earliest applications [14] of the "sum rules on the light-cone" was to the $D \rightarrow K^{(*)}$ form factors.

Also the strange quark mass entering the sum rule for $D \rightarrow K$ form factor has a smaller uncertainty than before. Furthermore, we use the improved determination [18] of the $SU(3)_{fl}$ violating Gegenbauer coefficient of the twist-2 kaon DA, and the updates of the pion and kaon twist-3,4 DA's from [19].

The main novelty in this paper concerns the q^2 -dependence of the form factors. First, we determine the slope parameters at $q^2 = 0$, which involve the second form factor $f_{D\pi(K)}^-$. The latter is calculated using the same method and input. Note that for $D \rightarrow \pi(K)$ transitions, LCSR's are applicable only in the lower part of the region $0 < q^2 < (m_D - m_{\pi(K)})^2$, accessible in the semileptonic $D \rightarrow \pi(K)\ell\nu_\ell$ decays. At q^2 approaching m_c^2 , the virtuality of the c -quark becomes a soft scale, and OPE is not reliable. In this paper we predict the form factor shapes, combining LCSR with analyticity. We employ the spacelike region $q^2 < 0$, where the light-cone OPE works even better, than at small positive q^2 . The LCSR results for the form factors at $q^2 < 0$ are fitted to various parameterizations, such as the dispersion relation with an effective pole [20] and the recent version of series parameterization [21]. We then make use of the analytic continuation from negative to positive q^2 and predict the form factors in the whole semileptonic region.

The paper is organized as follows. In Section 2 we present the outline of the method and discuss the expected accuracy of our calculation. In Section 3 the input parameters are listed and in Section 4 the numerical results for the form factors at zero momentum transfer are presented. In Section 5 we compare the calculated form factors with experimental data, and determine $|V_{cd}|$ and $|V_{cs}|$. In Section 6 we turn to the determination of the form factor shape and present the fit results for various parameterizations. The calculated shapes are used to predict the total semileptonic widths. Finally, Section 7 contains a concluding discussion. In Appendix A the relevant definitions of light-cone DA's and their expressions used in LCSR's are collected, and in Appendix B the formulae for the contributions to LCSR's are presented.

2. Outline of the LCSR method

The central objects of our interest are the $D \rightarrow \pi$ form factors $f_{D\pi}^\pm(q^2)$ defined in a standard way from the hadronic matrix element:

$$\langle \pi^-(p) | \bar{d}\gamma_\mu c | D^0(p+q) \rangle = 2f_{D\pi}^+(q^2)p_\mu + (f_{D\pi}^+(q^2) + f_{D\pi}^-(q^2))q_\mu, \quad (1)$$

and the analogous form factors $f_{DK}^\pm(q^2)$ of $D^0 \rightarrow K^-$ transition, obtained by replacing $d \rightarrow s$ and $\pi^- \rightarrow K^-$ in the above. In what follows, we work in the isospin symmetry limit, so that the $D^+ \rightarrow K^0$ and $D^0 \rightarrow K^-$ hadronic matrix elements are equal and the $D^+ \rightarrow \pi^0$ form factors are obtained by multiplying $f_{D\pi}^\pm(q^2)$ with $1/\sqrt{2}$. The form factor f^- is combined with f^+ in the scalar form factor

$$f_{D\pi(K)}^0(q^2) = f_{D\pi(K)}^+(q^2) + \frac{q^2}{m_D^2 - m_{\pi(K)}^2} f_{D\pi(K)}^-(q^2), \quad (2)$$

which plays a minor role in semileptonic transitions and is “visible” only in $D \rightarrow K\mu\nu_\mu$.

The correlation function used to derive LCSR's for $D \rightarrow \pi$ form factors is defined as

$$\begin{aligned} F_\mu^\pi(p, q) &= i \int d^4x e^{iq \cdot x} \langle \pi(p) | T \{ \bar{d}(x) \gamma_\mu c(x), m_c \bar{c}(0) i \gamma_5 u(0) \} | 0 \rangle \\ &= F^\pi(q^2, (p+q)^2) p_\mu + \tilde{F}^\pi(q^2, (p+q)^2) q_\mu. \end{aligned} \quad (3)$$

Replacing $d \rightarrow s$ and $\pi \rightarrow K$ in the above, we obtain F_μ^K , the correlation function for $D \rightarrow K$ form factors. The two invariant amplitudes $F^{\pi(K)}$ and $\tilde{F}^{\pi(K)}$ yield two separate sum rules for $f_{D\pi(K)}^+$ and $(f_{D\pi(K)}^+ + f_{D\pi(K)}^-)$, respectively. Using (2), one then obtains $f_{D\pi(K)}^0$, so that in our calculation, by default, $f_{D\pi(K)}^0(0) = f_{D\pi(K)}^+(0)$.

At $q^2 \ll m_c^2$ and $(p+q)^2 \ll m_c^2$, the c -quark propagating in the correlation function has a large virtuality and the product of the c -quark fields is expanded near the light-cone $x^2 \sim 0$. This expansion starts in leading order (LO) from the free c -quark propagator and includes the $O(\alpha_s)$ (NLO) corrections due to hard-gluon exchanges between the quark lines and soft-gluon emission. A more detailed derivation can be found e.g. in [9], where also the origin of the light-cone expansion in the correlation function is explained.

The OPE result for the correlation function (3) is cast in a factorized form, where the perturbatively calculable kernels are convoluted with the pion DA's of growing twist $t = 2, 3, 4, \dots$. For the invariant amplitude F^π one obtains:

$$\left[F^\pi(q^2, (p+q)^2) \right]_{OPE} = \sum_{t=2,3,4} F_0^{\pi,t}(q^2, (p+q)^2) + \frac{\alpha_s C_F}{4\pi} \sum_{t=2,3} F_1^{\pi,t}(q^2, (p+q)^2), \quad (4)$$

where the LO (NLO) parts in α_s are the convolutions

$$F_{0(1)}^{\pi,t}(q^2, (p+q)^2) = \int \mathcal{D}u T_{0(1)}^{(t)}(q^2, (p+q)^2, m_c^2, u, \mu) \phi_\pi^{(t)}(u, \mu). \quad (5)$$

The perturbative kernels $T_{0,1}^{(t)}$ stem from the c -quark propagator, and $T_1^{(t)}$ include the loops with hard-gluon exchanges in $O(\alpha_s)$. The pion DA's $\phi_\pi^{(t)}(u, \mu)$ represent universal vacuum-pion matrix elements of light-quark and gluon operators. The simplest bilocal quark-antiquark operators $\bar{d}(x) \Gamma^a u(0)$ (where Γ^a is a generic combination of γ -matrices) originate after contracting the free c -quark fields in the correlation function (3). In addition, soft gluons emitted from the propagating c -quark, together with light quarks and antiquarks, form DA's of higher multiplicity, starting from the three-particle (quark-antiquark-gluon) DA's of $t = 3, 4$. In (5), the integration over u is a generic notation for the momentum distribution between constituents of the pion in DA's. The definitions and explicit expressions for all relevant DA's are given in Appendix A. The presence of the terms with $2 \leq t \leq 4$ in (4) reflects the currently achieved accuracy in OPE: the twist 2,3,4 terms in LO (including three-particle contributions of twist 3,4) and the twist-2 and twist-3 (two-particle DA's) terms in NLO.

The factorization scale μ in (5) separates the perturbative kernels dominated by near light-cone distances from the long-distance quark-gluon dynamics in DA's. The collinear divergences in the twist-2 of OPE are absorbed in the logarithmic evolution of DA's as

shown in [10, 11]. The factorization for the twist-3 part is proved for the asymptotic DA's in [12] and confirmed in [13].

Note that the two terms in the c -quark propagator proportional to m_c and \not{p}_c yield two different parts of OPE with even ($t = 2, 4, \dots$) and odd ($t = 3, 5, \dots$) twists, respectively, corresponding to different chiralities of Γ^a matrices in the light-quark operators. Hence, the twist expansion goes in even and odd twists separately. The two most important LO contributions of twist-2 and twist-3 two-particle DA's to the correlation function originate from the $\sim m_c$ and $\sim \not{p}_c$ parts of the free c -quark propagator, respectively, and have simple expressions:

$$\begin{aligned}
F_0^{\pi,2}(q^2, (p+q)^2) &= f_\pi m_c^2 \int_0^1 \frac{du \varphi_\pi(u)}{m_c^2 - q^2 \bar{u} - (p+q)^2 u}, \\
F_0^{\pi,3[two\ part.]}(q^2, (p+q)^2) &= f_\pi \mu_\pi m_c \int_0^1 \frac{du}{m_c^2 - q^2 \bar{u} - (p+q)^2 u} \left\{ \phi_{3\pi}^p(u) \right. \\
&\quad \left. + \frac{1}{6} \left[2 + \frac{m_c^2 + q^2}{m_c^2 - q^2 \bar{u} - (p+q)^2 u} \right] \phi_{3\pi}^\sigma(u) \right\}, \quad (6)
\end{aligned}$$

where $\mu_\pi = m_\pi^2/(m_u + m_d)$ and $\bar{u} = 1 - u$. In the above, φ_π and $\phi_{3\pi}^p, \phi_{3\pi}^\sigma$ are the pion twist-2 and twist-3 two-particle DA's, respectively. Note that the formal $1/m_c$ suppression of $F_0^{\pi,3}$ versus $F_0^{\pi,2}$ is overwhelmed numerically, because the enhanced light-quark parameter μ_π is larger than m_c . The remaining twist-3 term in LO, due to the three-particle DA, not shown in (6), is strongly suppressed by the ratio of the small normalization factor $f_{3\pi}$ to m_c .

Turning to higher-twist ($t > 3$) contributions, one has to take into account that in the light-cone OPE each two units of twist are accompanied by an extra x^2 , yielding an additional power of the denominator

$$D = \frac{1}{m_c^2 - q^2 \bar{u} - (p+q)^2 u}, \quad (0 \leq u \leq 1), \quad (7)$$

in the correlation function. Hence, for example, the contribution $F_0^{\pi,4}$ of the twist-4 two- and three-particle DA's is subleading with respect to the twist-2 part $F_0^{\pi,2}$ in (6), with a suppression factor $\sim \delta_\pi^2 \langle D \rangle$, where $\langle D \rangle$ is the weighted (over DA's) average of the denominator (7), and $\delta_\pi^2 \sim \Lambda_{QCD}^2$ is the normalization factor of the twist-4 DA's. Similarly, the twist-5 contributions, not yet included in the currently used version (4) of OPE, are expected to be suppressed with respect to the twist-3 terms, parametrically $\sim \Lambda_{QCD}^2 \langle D \rangle$. We emphasize that the suppression of higher-twist contributions is effective only if both external momenta squared q^2 and $(p+q)^2$ in (7) are kept $\ll m_c^2$, that is, when the c -quark is sufficiently virtual.

The detailed calculation of the correlation function, including $O(\alpha_s)$ corrections to the twist-2 and twist-3 part, is given in previous papers and we will not repeat it. Here we use the recent update in terms of \overline{MS} heavy quark mass presented in [13], where m_b

has to be replaced by m_c , with a corresponding adjustment of the scales. As in [13], we use a universal normalization scale μ for α_s , quark masses and DA's. The u -, d -quark masses and m_π^2 are neglected everywhere, except in the parameter μ_π .

The correlation function F_μ^K for the $D \rightarrow K$ form factors includes $SU(3)_{fl}$ violation effects of different origin, starting from $O(m_s) \sim O(m_K^2)$. One effect is purely kinematical, due to the presence of $p^2 = m_K^2 \neq 0$ in the c -quark propagator. The expressions for the perturbative kernels have to be modified, so that the term $m_K^2 u\bar{u}$ has to be added to the denominator (7). Furthermore, there are $SU(3)_{fl}$ violating corrections in DA's. In twist 2, the deviations of φ_K from φ_π is due to differences between the normalization parameters (f_K vs f_π) and Gegenbauer moments. Importantly, one has to take into account the first Gegenbauer moment of the kaon DA, $a_1^K \neq 0$, responsible for the momentum distribution asymmetry between the strange quark and nonstrange antiquark in the kaon. In general, also $a_2^K \neq a_2^\pi$. In twist 3 and 4 DA's one has to replace the normalization parameters: $\mu_\pi \rightarrow \mu_K = m_K^2/(m_u + m_s)$, $f_{3\pi} \rightarrow f_{3K}$ and $\delta_\pi^2 \rightarrow \delta_K^2$, respectively. In addition, there are $O(m_K^2)$ admixtures of the twist-2 DA in the kaon DA's of twist 3 and 4. All these and some other less important $SU(3)_{fl}$ violating effects are included in the expressions for the kaon DA's [19] presented in Appendix A.

To access the $D \rightarrow \pi, K$ form factors, one equates the OPE result to the hadronic dispersion relation for the correlation function in the variable $(p+q)^2$, the momentum squared of the D -meson interpolating current. In the $D \rightarrow \pi$ case, the resulting relation for the invariant amplitude F^π is:

$$\left[F^\pi(q^2, (p+q)^2) \right]_{OPE} = \frac{2m_D^2 f_D f_{D\pi}^+(q^2)}{m_D^2 - (p+q)^2} + \frac{1}{\pi} \int_{s_0^D}^{\infty} ds \frac{\left[\text{Im} F^\pi(q^2, s) \right]_{OPE}}{s - (p+q)^2}. \quad (8)$$

In the above, the D -meson pole term (with the mass m_D and the decay constant defined as $\langle 0 | m_c \bar{q} i \gamma_5 c | D \rangle = m_D^2 f_D$), contains the desired form factor $f_{D\pi}^+$. Also in (8) the quark-hadron duality approximation is applied, replacing the hadronic spectral density of the higher states by the OPE spectral density. The latter approximation introduces the threshold parameter s_0^D which is non-universal and has to be determined for each sum rule independently. Note that s_0^D is an effective parameter, not necessarily equal to the lowest hadronic continuum threshold $(m_{D^*} + m_\pi)^2$.

After subtracting the integral on r.h.s. of (8) from both sides of this equation, one performs Borel transformation of (8) replacing the variable $(p+q)^2$ with the Borel parameter M^2 and exponentiating the denominators. E.g., the powers of the denominator D in (7) transform as:

$$\mathcal{B}_{(p+q)^2 \rightarrow M^2} \{ D^n \} = \frac{1}{(n-1)! u^n (M^2)^{n-1}} e^{-\frac{m_c^2 - q^2 \bar{u}}{u M^2}}. \quad (9)$$

Finally, the LCSR for the $D \rightarrow \pi$ form factor is obtained:

$$f_{D\pi}^+(q^2) = \frac{e^{m_D^2/M^2}}{2m_D^2 f_D} \left(\sum_{t=2,3,4} F_0^{\pi,t}(q^2, M^2, s_0^D) + \frac{\alpha_s C_F}{4\pi} \sum_{t=2,3} F_1^{\pi,t}(q^2, M^2, s_0^D) \right), \quad (10)$$

where the functions $F_0^{\pi,t}(q^2, M^2, s_0^D)$ and $F_1^{\pi,t}(q^2, M^2, s_0^D)$ are derived applying the Borel-and-subtraction procedure to each twist component of the OPE in (4):

$$F_{0(1)}^{\pi,t}(q^2, M^2, s_0^D) = \mathcal{B}_{(p+q)^2 \rightarrow M^2} \left\{ F_{0(1)}^{\pi,t}(q^2, (p+q)^2) \right\} - \frac{1}{\pi} \int_{s_0^D}^{\infty} ds e^{-s/M^2} \text{Im} F_{0(1)}^{\pi,t}(q^2, s). \quad (11)$$

The expressions for $F_0^{\pi,t}$ and $F_1^{\pi,t}$ in (10) are obtained from the corresponding expressions given in [13] for $B \rightarrow \pi$ LCSR, replacing $b \rightarrow c$ and $B \rightarrow D$. The second LCSR for the combination $(f_{D\pi}^+ + f_{D\pi}^-)$ is obtained from the invariant amplitude \tilde{F}^π and has the same form as (10), with the invariant amplitudes $\tilde{F}_{0(1)}^{\pi,t}$, replacing $F_{0(1)}^{\pi,t}$, and without the factor 1/2 in the coefficient.

For $D \rightarrow K$ form factors, as explained above, the $SU(3)_{fl}$ violation effects are taken into account in both LCSR's for f_{DK}^+ and $(f_{DK}^+ + f_{DK}^-)$ in the LO part, keeping $p^2 = m_K^2 \neq 0$ in the hard kernels and taking into account the $O(m_s) \sim O(m_K^2)$ effects in the kaon DA's. For the sake of completeness, we do not expand these expressions in $m_K^2 \sim m_s$, although it is clear that only the first-order terms of this expansion are important numerically. Furthermore, having in mind that both $O(\alpha_s)$ and $O(m_s)$ corrections are reasonably small, we do not take into account the combined $O(\alpha_s m_s)$ effects, originating from nonzero m_s and $p^2 = m_K^2$ in the NLO diagrams. These effects demand a dedicated calculation, taking into account the mixing between various twist components at the $O(m_s)$ level. Hence, in the adopted approximation $F_1^{K,2(3)} = F_1^{\pi,2(3)}$.

In Appendix B, we present the expressions for all LO terms $F_0^{K,t=2,3,4}$ entering LCSR's for $D \rightarrow K$ form factors. In the limit $m_s \rightarrow 0$ ($m_K^2 \rightarrow 0$) and $\mu_K \rightarrow \mu_\pi$ the corresponding terms $F_0^{\pi,t=2,3,4}$ in the $D \rightarrow \pi$ LCSR's are easily reproduced. The expressions for the NLO terms of twist-2 and twist-3 are presented in [13] in a form of dispersion integrals, and we replace $m_b \rightarrow m_c$. These very bulky formulae are not displayed here.

The LCSR's for $D \rightarrow K$ form factors were also compared to the recent update of the LCSR's for $B \rightarrow K$ form factors presented in [22]. The expressions presented in Appendix B agree with those in [22], up to the twist-3 three-particle part of LCSR, which is incomplete in [22]. We also modified the m_K^2 -corrections to the two-particle twist-4 DA's (see discussion in Appendix A), hence, there are small differences in the corresponding twist-4 terms in LCSR's. Both differences have a minor impact on numerical results. Finally, we compared our expressions with the LCSR for the $D \rightarrow P$ ($P = \pi, K$) form factor in LO at $q^2 = 0$ presented in [16], where only the $O(m_P^2)$ terms are retained. In the limit $m_P^2 = 0$, the equations (75), (76), and (77) are reduced to the corresponding terms in Eq. (2) of [16], except we obtain an opposite sign of the contribution of twist-4 DA $\psi_{4;P}$. We also were not able to completely reproduce the $O(m_P^2)$ terms in this equation.

The expected accuracy of LCSR (10) is determined by the uncertainties of the combined expansion in twists and α_s of the correlation function. The choice of Borel parameter plays an important role here. Note that Borel transformation effectively replaces the powers of the denominator D in the higher-twist contributions by the inverse pow-

ers of M^2 , as seen from (9)². Hence, although M^2 is an arbitrary scale, it should be taken sufficiently large to preserve the twist hierarchy. Parametrically, in the limit of the heavy c -quark mass, the relevant scaling relation is $M^2 \sim 2m_c\tau$. Importantly, also the scale τ has to be much larger than the typical soft scales of $O(\Lambda_{QCD})$, such as the normalization parameters of higher-twist DA's. The twist expansion is then “protected” by the combinations of $1/m_c$ and $1/\tau$ suppression factors, as one can explicitly prove by expanding LCSR in powers of $1/m_c$ (for more details on heavy-quark expansion of LCSR see [11, 23, 24]).

Another important step in the derivation of LCSR is the subtraction of the integral over higher states in (11). This procedure introduces the lower limit $u_0 = (m_c^2 - q^2)/(s_0^D - q^2)$ in the convolution integrals entering LCSR (see the expressions for $F_0^{K,t}(q^2, M^2, s_0^D)$ in Appendix B). In LCSR's for $D \rightarrow \pi, K$ form factors the integration limit is $u_0 \simeq 0.3 - 0.4$. Hence, the suppression of higher twists is not influenced, because after subtraction, the large part of the u -region in the integrals over DA's is retained. This is not the case in the limit of infinitely heavy quark and small q^2 , when, according to the scaling rule, $s_0^D \sim (m_c^2 + 2m_c\omega)$ and $u_0 \sim 1 - 2\omega/m_c \rightarrow 1$. In this limit the power suppression of the higher-twist terms in LCSR depends also on the end-point behavior of DA's, modifying the initial twist hierarchy of OPE. For example, the formal $1/m_c$ suppression of the twist-3 terms mentioned above, is removed at $m_c \rightarrow \infty$. Still, this modification does not influence the numerical suppression of $t \geq 4$ contributions, provided the effective Borel scale τ is kept large.

The accuracy of the quark-hadron duality approximation is difficult to estimate in a model-independent way. In LCSR, one minimizes the sensitivity to this approximation, using not too large M^2 , in order to suppress the integral over the higher states exponentially. In addition, the effective threshold s_0^D is determined, calculating the D -meson mass from the differentiated LCSR (10) and adjusting the result to the measured value, as it was done in [12, 13]. This procedure is more reliable than fixing the effective threshold from a stability of the sum rule with respect to the Borel parameter variation. On the other hand, if the result of LCSR calculation actually reveals a weak dependence on M^2 (within the adopted interval), that is an important indication of the reliability of the method.

3. Choice of the input

In this section we specify and discuss the choice of input parameters entering LCSR's. As already mentioned, we use the \overline{MS} scheme for the quark masses. In previous analyses, (e.g., in [15, 16]) the c -quark pole mass was used in the final sum rule, which is certainly less convenient for a correlation function with a virtual c quark. For the c -quark mass value we adopt the interval obtained from charmonium sum rules with $O(\alpha_s^3)$ accuracy [17],

$$\bar{m}_c(\bar{m}_c) = (1.29 \pm 0.03) \text{ GeV}, \quad (12)$$

²The LCSR expressions in Appendix B are given in a compact form, using derivatives of DA's. To restore the inverse powers of M^2 one has to perform a partial integration.

where, conservatively, we double the error. This interval is in a good agreement with the recent lattice determination [25]. For the s -quark mass we take the interval

$$m_s(\mu = 2 \text{ GeV}) = (98 \pm 16) \text{ MeV}, \quad (13)$$

which covers the range of the QCD sum rule determinations with $O(\alpha_s^4)$ accuracy [26]. Employing the well known ChPT relations [27]:

$$R = \frac{2m_s}{m_u + m_d} = 24.4 \pm 1.5, \quad Q^2 = \frac{m_s^2 - (m_u + m_d)^2/4}{m_d^2 - m_u^2} = (22.7 \pm 0.8)^2, \quad (14)$$

the u, d -quark masses and their sum can be calculated. Since we neglect m_u and m_d everywhere, except in the parameters μ_π and μ_K , we simply use the above relations and obtain (adding the errors in quadrature):

$$\begin{aligned} \mu_\pi(2 \text{ GeV}) &= \frac{m_\pi^2 R}{2m_s(2 \text{ GeV})} = (2.43 \pm 0.42) \text{ GeV}, \\ \mu_K(2 \text{ GeV}) &= \frac{m_K^2}{m_s(2 \text{ GeV}) \left[1 + \frac{1}{R} \left(1 - \frac{R^2 - 1}{4Q^2} \right) \right]} = (2.42 \pm 0.39) \text{ GeV}, \end{aligned} \quad (15)$$

with a remarkably small $SU(3)_{fl}$ violation.

In our numerical analysis, the two-loop running for QCD coupling is used, with $\alpha_s(m_Z) = 0.1176 \pm 0.002$ [28]. The scale-dependence of the quark masses and parameters of DA's is taken into account in one-loop approximation. Furthermore, we use a uniform scale μ for all renormalizable parameters, with the same default value $\mu = 1.4 \text{ GeV}$, as in previous analyses of LCSR's; note that parametrically, $\mu \sim \sqrt{m_D^2 - m_c^2}$.

The hadronic inputs in LCSR's include the hadron masses $m_{D^0} = 1.865 \text{ GeV}$, $m_{\pi^\pm} = 139.6 \text{ MeV}$ and $m_{K^\pm} = 493.7 \text{ MeV}$ [28]. The pion and kaon decay constants, $f_\pi = 130.4 \text{ MeV}$ and $f_K = 155.5 \text{ MeV}$ [28] normalize the twist-2 pion and kaon DA's, respectively. All other parameters of twist 2,3,4 DA's relevant for our calculation are collected in Table 5 in Appendix A. Let us briefly comment on our choice. Expressing the twist-2 DA's in terms of Gegenbauer polynomials, we adopt the intervals $a_2^\pi(1 \text{ GeV}) = 0.16 \pm 0.01$, $a_4^\pi(1 \text{ GeV}) = 0.04 \pm 0.01$, determined in [13], by fitting the form factor calculated from LCSR to the measured shape of $B \rightarrow \pi$ form factor. These intervals are in agreement with the other determinations of $a_{2,4}^\pi$ summarized in [19]. For the first Gegenbauer moment of the kaon DA we use $a_1^K = 0.10 \pm 0.04$, obtained in [18] from the two-point QCD sum rules with NNLO accuracy. Finally, the interval $a_2^K = 0.25 \pm 0.15$ is adopted [29, 19]. All other Gegenbauer moments are put to zero, the same approximation as in the previous LCSR analyses. In fact, as already noticed in [16], the sensitivity of the LCSR for the $D \rightarrow \pi$ form factor to Gegenbauer moments is less than in the $B \rightarrow \pi$ case. In particular, we have checked that nonvanishing values of the next Gegenbauer moments a_3^K and a_4^K , at the level of a_1^K and a_4^π , respectively, have a small influence on the numerical results. For the twist-3,4 pion and kaon DA's, in addition to the normalization parameters already specified in (15) the set of parameters

determined and updated in [19] is used. Note that due to the smallness of $f_{3\pi} \simeq f_{3K}$, the size of nonasymptotic corrections to the twist-3 DA's $\phi_{3\pi,3K}^{p,\sigma}$ is small. Hence, it is justified to take asymptotic DA's in the NLO twist-3 terms of LCSR calculated in [12, 13].

The remaining hadronic input in LCSR (10) is the decay constant f_D . In previous applications of LCSR's to heavy-light form factors, e.g., in [12, 13, 15], the two-point QCD sum rule for the heavy-meson decay constant was substituted in LCSR, leading to a partial cancellation between radiative gluon corrections. However, the two-point sum rule, with its own Borel-parameter range and effective duality threshold, introduces an additional uncertainty in the calculated form factors. Note that in the sum rules with \overline{MS} heavy-quark mass the α_s -corrections are not sizeable and, therefore, their partial cancellation is not that important. On the other hand, the decay constant f_D has already been measured in $D \rightarrow l\nu_l$ [30] with a very good accuracy. For that reason, in our numerical analysis we prefer to use the experimental result, assuming the isospin symmetry: $f_{D^0} = f_{D^\pm}$, and taking $f_{D^+} = 205.8 \pm 8.9$ MeV from [30], where we add the errors in quadrature. Importantly, this value is obtained assuming $|V_{cd}| = |V_{us}|$, with $|V_{us}| = 0.2255 \pm 0.0019$ from [28]. Extracting $|V_{cd}|$ below, we will take this into account. The two-point QCD sum rule prediction for f_D used in previous analyses (e.g., in [15]) agrees with the experimental interval, but has a larger uncertainty.

Finally, we specify the ‘‘internal’’ parameters of LCSR (10): the interval of the Borel parameter M^2 and the effective threshold s_0^D . For the former, we choose the region $M^2 = (4.5 \pm 1.0)$ GeV², close to the one used in [15]. The threshold parameter $s_0^D = (7.0 \pm 0.5)$ GeV² is fixed by reproducing (within 2% accuracy) the D -meson mass from the auxiliary sum rule, obtained from differentiating the LCSR (10) over $1/M^2$ and dividing the result by (10). With our choice of M^2 and s_0^D , the usual criteria are fulfilled for the LCSR (10): smallness of the subleading twist-4 contributions ($< 5\%$ of the twist-2 term) and, simultaneously, suppression of higher state contributions ($< 10\%$ of the total correlation function). Since below we also calculate the form factors at negative q^2 , we checked that the adopted ranges of M^2 and s_0^D are equally applicable for -2 GeV² $\leq q^2 \leq 0$. For the second LCSR for $(f_{D\pi}^+ + f_{D\pi}^-)$, the same intervals are taken for consistency. The differences between the Borel and threshold parameters for the sum rules for $D \rightarrow \pi$ and $D \rightarrow K$ form factors turn out to be negligible. Note also that the effective Borel scale $\tau = M^2/(2m_c) \simeq 1.7$ GeV is sufficiently large.

4. Form factors at $q^2 = 0$

Substituting in LCSR (10) the input specified above, we calculate the form factors $f_{D\pi}^+(0)$ and $f_{DK}^+(0)$. The numerical evaluation was done in two different ways: firstly by a direct integration over imaginary parts of hard-scattering amplitudes, and secondly, applying the numerically equivalent method of analytical continuation explained and used in [13, 22].

The results at the central values of input parameters are displayed in Table 1. Their dependence on Borel parameter is shown in Fig. 1, and exhibits a remarkable stability,

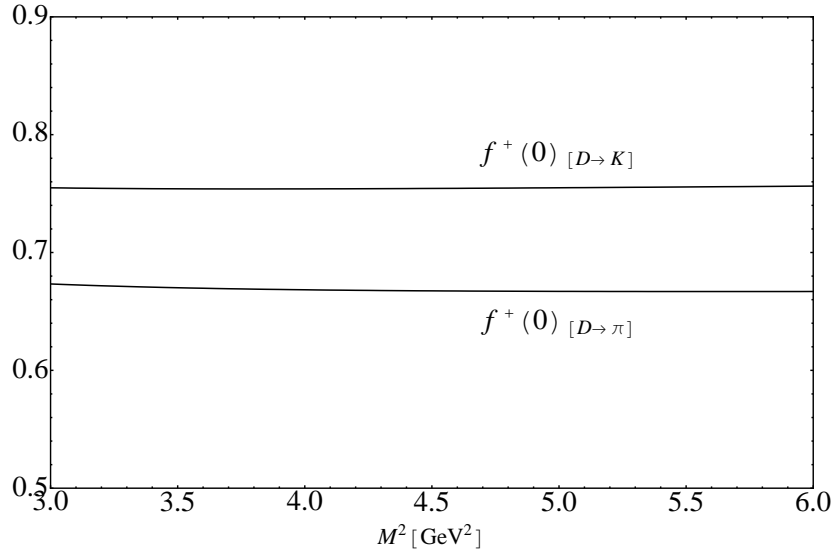


Figure 1: *The Borel-parameter dependence of the form factors $f_{D\pi}^+(0)$ and $f_{DK}^+(0)$ calculated from LCSR.*

even beyond the adopted interval. The scale-dependence displayed in Fig. 2, is also mild. Conservatively, we consider the variation of the calculated form factors with the scale change in the interval $1.0 < \mu < 3.0$ GeV as one of the uncertainties. In addition, we investigate the numerical hierarchy of various contributions to LCSR. The sample of results for $f_{D\pi}^+(q^2)$ and $f_{DK}^+(q^2)$ is collected in Table 2. The dominance of the twist-3 LO contribution was anticipated, due to the factor $\mu_\pi/m_c > 1$. At the same time, the subleading twist-4 contributions are numerically strongly suppressed. The NLO corrections to twist-2,3 terms are also small, a clear indication that the "soft-overlap" mechanism dominates in $D \rightarrow \pi, K$ form factors.

Furthermore, we estimate separate uncertainties of our calculation by varying each input parameter within its allowed interval. All significant uncertainties of $f_{D\pi(K)}^+(0)$

Table 1: *Form factors $f_{D\pi}^+(0)$ and $f_{DK}^+(0)$ calculated from LCSR (10) and the estimated uncertainties due to the variation of the input.*

Formf. centr.value	M^2	μ	s_0^D	$(f_D)_{exp}$	m_c	m_s $\mu_{\pi,K}$	Gegenbauer moments	tw.5 (est.)
$f_{D\pi}^+(0)$ 0.667	+0.003 -0.001	+0.04 -0.003	± 0.01	± 0.03	+0.005 -0.006	+0.08 -0.06	± 0.001 ($a_{2,4}^\pi$)	± 0.017
$f_{DK}^+(0)$ 0.754	+0.001 -0.0004	+0.04 -0.006	± 0.01	± 0.03	+0.005 -0.007	+0.09 -0.06	± 0.003 (a_1^K) ± 0.03 (a_2^K) ± 0.01 ($a_{3,4}^K$)	± 0.001

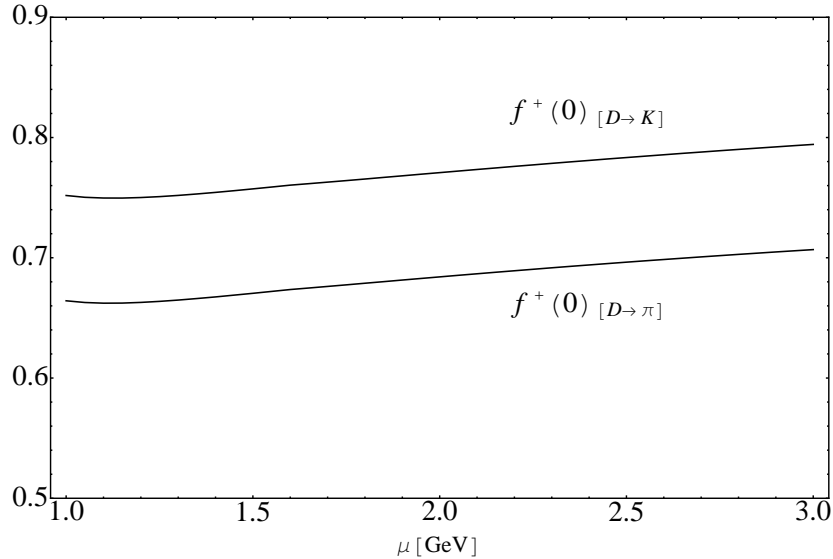


Figure 2: *The scale-dependence of the form factors $f_{D\pi}^+(0)$ and $f_{DK}^+(0)$ calculated from LCSR*

Table 2: *Relative contributions to LCSR for the form factors $f_{D\pi}^+(q^2)$ and $f_{DK}^+(q^2)$*

Contribution	$f_{D\pi}^+(0)$	$f_{D\pi}^+(q^2 = -2 \text{ GeV}^2)$	$f_{DK}^+(0)$	$f_{DK}^+(q^2 = -2 \text{ GeV}^2)$
tw2 LO	35.9%	32.9%	36.2%	33.7%
tw2 NLO	6.3%	8.4%	6.0%	7.9%
tw3 LO	66.0%	59.5%	67.9%	58.9%
tw3 NLO	-9.5%	-2.9%	-10.1%	-2.9%
tw4 LO	1.4%	2.2%	-0.07%	2.4%

are collected in Table 1. (For brevity we do not show a similar table for $f_{D\pi(K)}^+(0) + f_{D\pi(K)}^-(0)$, presenting only the total uncertainty below.) The remaining small effects, e.g., due to the variation of α_s , are not shown, but included in the total uncertainty. Note that, according to (15), the error related to both μ_π and μ_K is influenced by the uncertainties in the determination of m_s and ChPT parameters. To roughly estimate the effects of the unknown twist-5 contributions to LCSR's, we assume that their ratio to the twist-3 contribution is equal to the calculated ratio of twist-4 and twist-2 (LO) terms. Since in the sum rules for $f_{D\pi(K)}^+ + f_{D\pi(K)}^-$ there is no LO twist-2 contribution, we conservatively assume that the magnitudes of the twist-5 and twist-4 terms are the same. In addition, to assess the effect of higher Gegenbauer moments a_3^K and a_4^K on the $D \rightarrow K$ form factor, we recalculated this form factor assuming $a_3^K = \pm a_1^K$ and $a_4^K = \pm a_4^\pi$. The small variations due to the abovementioned effects are treated as separate uncertainties and included in the error budget in Table 1.

Adding all uncertainties in quadrature, we obtain:

$$f_{D\pi}^+(0) = 0.67_{-0.07}^{+0.10}, \quad (16)$$

$$f_{DK}^+(0) = 0.75_{-0.08}^{+0.11}. \quad (17)$$

The second LCSR yields numerical results for the sums of the form factors:

$$f_{D\pi}^+(0) + f_{D\pi}^-(0) = 0.46_{-0.09}^{+0.12}, \quad (18)$$

$$f_{DK}^+(0) + f_{DK}^-(0) = 0.60_{-0.09}^{+0.12}, \quad (19)$$

We also quote our prediction for the products of D decay constant and the form factors:

$$f_D f_{D\pi}^+(0) = 137_{-14}^{+19} \text{ MeV}, \quad (20)$$

$$f_D f_{DK}^+(0) = 155_{-15}^{+21} \text{ MeV}. \quad (21)$$

These quantities are independent of the experimental value of f_D , used to calculate (16) and (17), and therefore have a slightly smaller uncertainty.

Finally, the predicted ratio of the form factors is

$$\frac{f_{D\pi}^+(0)}{f_{DK}^+(0)} = 0.88 \pm 0.05, \quad (22)$$

where the f_D dependence drops out and some uncertainties largely cancel.

In Table 3 we compare theoretical predictions for the form factors $f_{D\pi}^+(0)$ and $f_{DK}^+(0)$, obtained in lattice QCD and from LCSR's. Our results are in a good agreement with the lattice determinations. The form factors (16) and (17) and their ratio (22) are also in accordance with the previous LCSR estimates [15, 16]. The $D \rightarrow K$ form factor is now more accurately determined than in [15], due to a better knowledge of the c - and s -quark masses and of the parameter a_1^K .

In the final part of this section we present our predictions for the slopes and ratios of the form factors at $q^2 = 0$, that is, at large recoil of the pion or kaon, (see [34]

Table 3: *Comparison of theoretical predictions for the form factors $f_{D\pi}^+(0)$ and $f_{DK}^+(0)$.*

Method	[Ref.]	$f_{D\pi}^+(0)$	$f_{DK}^+(0)$
Lattice QCD	[31]	$0.57 \pm 0.06 \pm 0.02$	$0.66 \pm 0.04 \pm 0.01$
	[32]	$0.64 \pm 0.03 \pm 0.06$	$0.73 \pm 0.03 \pm 0.07$
	[33]	$0.74 \pm 0.06 \pm 0.04$	$0.78 \pm 0.05 \pm 0.04$
LCSR	[15]	0.65 ± 0.11	$0.78_{-0.15}^{+0.2}$
	[16]	0.63 ± 0.11	0.75 ± 0.12
	this work	$0.67_{-0.07}^{+0.10}$	$0.75_{-0.08}^{+0.11}$

for definition). We start with the parameter δ for $D \rightarrow \pi$ transitions, which is simply calculated by taking the ratio of two LCSR's:

$$\delta_{D\pi} = 1 + \frac{f_{D\pi}^-(0)}{f_{D\pi}^+(0)} = 0.69 \pm 0.09. \quad (23)$$

The slope of the scalar form factor at $q^2 = 0$ normalized by $f_{D\pi}^+(0)$ is another interesting characteristics of the form factor. We obtain:

$$\beta_{D\pi} = \left[\left(\frac{m_D^2 - m_\pi^2}{f_{D\pi}^+(0)} \right) \frac{df_{D\pi}^0(q^2)}{dq^2} \Big|_{q^2=0} \right]^{-1} = 1.4 \pm 0.3. \quad (24)$$

Combining these two parameters, we are able to predict the combination

$$1 + 1/\beta_{D\pi} - \delta_{D\pi} = 1.02 \pm 0.18, \quad (25)$$

consistent with the CLEO measurement [2]: $1 + 1/\beta_{D\pi} - \delta_{D\pi} = 0.93 \pm 0.09 \pm 0.01$. The corresponding slope parameters for $D \rightarrow K$ form factors predicted from LCSR are:

$$\delta_{DK} = 0.79 \pm 0.07, \quad \beta_{DK} = 1.6 \pm 0.4, \quad (26)$$

so that

$$1 + 1/\beta_{DK} - \delta_{DK} = 0.84 \pm 0.17 \quad (27)$$

also agrees with the experimental result [2]: $1 + 1/\beta_{DK} - \delta_{DK} = 0.89 \pm 0.04 \pm 0.01$.

As discussed in the literature (see e.g, [34]), the values of δ and β for heavy-light form factors reflect the proportion of their hard-scattering and soft-recoil components and, respectively, their deviation from the scaling behavior predicted in the combined heavy-quark and large-recoil limit. We postpone a more detailed discussion of these parameters to a future study.

5. Determination of $|V_{cd}|$ and $|V_{cs}|$

The latest CLEO measurements of semileptonic charm decays [2], fitted to various form factor parameterizations (to be discussed in detail in the next section), yield the products $f_{D\pi}(0)|V_{cd}|$ and $f_{DK}(0)|V_{cs}|$. Both CKM matrix elements can now be determined using our predictions for the form factors $f_{D\pi}(0)$ and $f_{DK}(0)$.

Having an accurate experimental value for f_D at our disposal, allows us to make the extraction of $|V_{cd}|$ less dependent on the theoretical uncertainty of LCSR, than in previous analyses, where a sum rule prediction for f_D was used. We employ the CLEO result [30] for the D -meson decay constant multiplied by $|V_{cd}|$, (i.e, without the additional assumption $|V_{cd}| = |V_{us}|$):

$$f_D|V_{cd}| = 46.4 \pm 2.0 \text{ MeV}. \quad (28)$$

On the other hand, the CLEO result [2] for the same CKM matrix element multiplied by the form factor is :

$$f_{D\pi}(0)|V_{cd}| = 0.150 \pm 0.004 \pm 0.001, \quad (29)$$

obtained from the fit of the q^2 -bins in $D \rightarrow \pi e \nu$ in a form of the series parameterization. The product of the above two experimental numbers is then divided by the LCSR prediction (20), yielding $|V_{cd}|^2$, from which we obtain:

$$|V_{cd}| = 0.225 \pm 0.005 \pm 0.003 \begin{matrix} +0.016 \\ -0.012 \end{matrix}, \quad (30)$$

where the first and second errors originate from the experimental errors in (28) and (29), respectively, and the third error is due to the uncertainty of LCSR. Note that this procedure involves the square of $|V_{cd}|$ on the experimental side. Hence, the theoretical uncertainty of LCSR given in (20) approximately halves in (30). Our result is in a good agreement with the value $|V_{cd}| = 0.234 \pm 0.007 \pm 0.002 \pm 0.025$ determined in [2] by using the lattice QCD value of $f_{D\pi}^+(0)$ from [32]. This agreement is not surprising because the form factor obtained from LCSR is close to the lattice result (see Table 3).

Furthermore, we determine the ratio of $|V_{cd}|$ to $|V_{cs}|$, dividing (29) by

$$f_{DK}(0)|V_{cs}| = 0.719 \pm 0.006 \pm 0.005, \quad (31)$$

obtained from $D \rightarrow K e \nu_e$ data fit [2]. Using the ratio (22) we obtain:

$$\frac{|V_{cd}|}{|V_{cs}|} = 0.236 \pm 0.006 \pm 0.003 \pm 0.013, \quad (32)$$

where the first and second uncertainties are due to the combined (in quadratures) errors in (29) and (31), respectively, and the third uncertainty stems from the LCSR calculation. Within errors, this ratio is in agreement with $|V_{cd}|/|V_{cs}|$ obtained from the values quoted in [2], where $|V_{cs}| = 0.985 \pm 0.009 \pm 0.006 \pm 0.103$ was determined using the form factor $f_{DK}^+(0)$ from lattice QCD [32]. Our determinations (30) and (32) are consistent with $|V_{cd}| = |V_{us}|$ and $|V_{cs}| = |V_{ud}|$.

6. Form factors and their shapes at $q^2 \neq 0$

The form factors $f_{D\pi}^+(q^2)$ and $f_{DK}^+(q^2)$ are analytic functions of the complex variable q^2 . The singularities located on the real positive axis include the poles of the ground-state vector mesons D^* and D_s^* , respectively, and their radially excited states. In addition, there are branch points, generated by the hadronic continuum states, starting from $D\pi$ and DK thresholds at $q^2 = (m_D + m_\pi)^2$ and $q^2 = (m_D + m_K)^2$, respectively. (Note that the $D_s\pi$ intermediate state in the $D \rightarrow K$ form factor is forbidden in the isospin limit). To obtain convenient parameterizations for the form factors, one employs analyticity in two different ways.

The first approach uses the dispersion relation, e.g., for the $D \rightarrow \pi$ form factor:

$$f_{D\pi}^+(q^2) = \frac{c_{D^*}}{1 - q^2/m_{D^*}^2} + \int_{(m_D+m_\pi)^2}^{\infty} ds \frac{\rho_h^{D\pi}(s)}{s - q^2}, \quad (33)$$

where the ground-state D^* -pole at $m_{D^*}^2 = (2.01 \text{ GeV})^2$ [28] is isolated, and the hadronic spectral density $\rho_h^{D\pi}(s)$ includes all other intermediate hadronic states with the D^*

quantum numbers. In fact, $m_{D^*}^2$ is slightly larger than the continuum threshold (so that the $D^* \rightarrow D\pi$ decay is observable), whereas in the dispersion relation for $f_{DK}^+(q^2)$ the D_s^* pole at $m_{D_s^*}^2 = (2.112 \text{ GeV})^2$ [28] lies below the threshold. Importantly, the dispersion relation (33) has no subtractions, due to the expected QCD asymptotics of the form factor $\lim_{|q^2| \rightarrow \infty} f_{D\pi}^+(q^2) \sim 1/|q^2|$. The residue of the pole in (33) is normalized as:

$$c_{D^*} = \frac{f_{D^*} g_{D^* D\pi}}{2m_{D^*}}, \quad (34)$$

where f_{D^*} and $g_{D^* D\pi}$ are the D^* decay constant and $D^* D\pi$ strong coupling, respectively, defined in the standard way (see e.g., [9]).

The rigorous dispersion relation (33) is valid at any q^2 . Hence, matching a calculated form factor, e.g., the one obtained from LCSR, to the dispersion relation in the region where this calculation is valid, one can, in principle, predict the form factor outside this region. This is, however, only possible, if the complicated integral over the hadronic spectral density in (33) is parameterized in a simple and reliable way. One possibility is to replace this integral by an effective pole:

$$f_{D\pi}^+(q^2) = c_{D^*} \left(\frac{1}{1 - q^2/m_{D^*}^2} - \frac{\alpha_{D\pi}}{1 - q^2/(\gamma_{D\pi} m_{D^*}^2)} \right), \quad (35)$$

where $\alpha_{D\pi}$ and $\gamma_{D\pi}$ parameterize the residue and the position of this pole, so that the normalization of the form factor at $q^2 = 0$ is:

$$f_{D\pi}^+(0) = c_{D^*} (1 - \alpha_{D\pi}). \quad (36)$$

Using the relation $\gamma_{D\pi} = 1/\alpha_{D\pi}$ inspired by the combined heavy-quark and large-recoil limit, the two-pole ansatz is reduced [20] to the specific BK-parameterization:

$$f_{D\pi}^+(q^2) = \frac{f_{D\pi}^+(0)}{(1 - q^2/m_{D^*}^2)(1 - \alpha_{D\pi} q^2/m_{D^*}^2)}. \quad (37)$$

The second approach based on the analyticity of the form factors employs the conformal mapping of the q^2 -plane (see e.g., [35] for the early uses):

$$z(q^2, t_0) = \frac{\sqrt{t_+ - q^2} - \sqrt{t_+ - t_0}}{\sqrt{t_+ - q^2} + \sqrt{t_+ - t_0}}, \quad (38)$$

where $t_{\pm} = (m_D \pm m_{\pi(K)})^2$ and $t_0 < t_+$ is an auxiliary parameter. Applying this transformation, one maps the q^2 -plane (with a cut along the positive axis) onto the inner part of the unit circle in the z plane, so that $f_{D\pi(K)}^+(q^2)_{q^2 \rightarrow z}$ is free from singularities at $|z| < 1$. The conformal mapping (38) was employed while deriving the unitarity bounds for the heavy-light form factors in [36, 37]. Independent of these bounds, with an optimal choice of t_0 , the semileptonic region $0 < q^2 < (m_D - m_{\pi(K)})^2$ is mapped onto the interval of small $|z|$. Hence, a simple expansion in powers of z around $z = 0$, retaining only a few first terms, provides a reasonably accurate parameterization of the form factor.

In this paper we will use the recently suggested version [21] of the series parameterization for $B \rightarrow \pi$ form factor. Adapting it to the case of $D \rightarrow \pi$ transition, we have:

$$f_{D\pi}^+(q^2) = \frac{1}{1 - q^2/m_{D^*}^2} \sum_{k=0}^N \tilde{b}_k [z(q^2, t_0)]^k. \quad (39)$$

As explained in [21], this parameterization ensures general analytic properties of the form factor: the D^* -pole, branch point at $q^2 = t_+$ and $\sim 1/q^2$ asymptotics at large q^2 . Furthermore, to obey the expected near-threshold behaviour, the relation

$$\tilde{b}_N = -\frac{(-1)^N}{N} \sum_{k=0}^{N-1} (-1)^k k \tilde{b}_k \quad (40)$$

has to be introduced, reducing the number of independent parameters by one. In addition, we find it more convenient to keep the form factor at zero momentum transfer $f_{D\pi}^+(0)$ as one of the independent parameters, correspondingly rescaling the coefficients in the series expansion: $\tilde{b}_k = f_{D\pi}^+(0)b_k$, so that

$$b_0 = 1 - \sum_{k=1}^{N-1} b_k \left[z(0, t_0)^k - (-1)^{k-N} \frac{k}{N} z(0, t_0)^N \right]. \quad (41)$$

This leads to the final form of the series parameterization used in our analysis:

$$f_{D\pi}^+(q^2) = \frac{f_{D\pi}^+(0)}{1 - q^2/m_{D^*}^2} \left\{ 1 + \sum_{k=1}^{N-1} b_k \left(z(q^2, t_0)^k - z(0, t_0)^k - (-1)^{k-N} \frac{k}{N} \left[z(q^2, t_0)^N - z(0, t_0)^N \right] \right) \right\}. \quad (42)$$

In [21] the advantages of this choice with respect to the previous versions [36] are discussed (see also [38]). The analogous ansatz for f_{DK}^+ contains $m_{D_s^*}^2$ in the pole prefactor. Note that the formal prescription for the conformal mapping is to multiply the r.h.s. of (42) by the pole factor if the ground-state pole lies below the threshold t_+ , which is, strictly speaking, only valid for $D \rightarrow K$ form factor. We prefer to retain this factor in (42) also for $D \rightarrow \pi$ case, having in mind that D^* is located very close to the $D\pi$ threshold. In what follows, we simply rely on the smallness of the variable z in (42), not taking into account the unitarity bounds [36] for the coefficients b_k , because, at least for small N , these bounds are not restrictive [21] (see also [37]).

In order to match the LCSR prediction for $D \rightarrow \pi$ and $D \rightarrow K$ form factors to one of the parameterizations discussed above, we have to calculate these form factors beyond $q^2 = 0$. However, the small part $0 \leq q^2 \ll m_c^2$ of the semileptonic region where our calculation is valid, is too narrow to serve as a "lever arm" for fitting various parameterizations.

In this work, in order to enlarge the interval of q^2 , we calculate the form factors at $q_{min}^2 < q^2 < 0$, that is, at negative momentum transfers not accessible in semileptonic

decays³. Fitting the LCSR predictions in this region to a certain parameterization, we then use the analyticity of the form factors, continuing the fitted parameterization to positive q^2 and accessing the whole semileptonic region $0 \leq q^2 < t_-$.

Note that LCSR's are fully applicable at $q^2 < 0$, since the virtuality of the c quark in the correlation function is even larger at $q^2 < 0$, than at $q^2 = 0$. For our purpose it is sufficient to take q^2 not too large, and the actual numerical calculation is done up to $q_{min}^2 = -2 \text{ GeV}^2$. In fact, there are several reasons to keep moderate values of $|q^2|$. First, we still can use the same ranges of the sum rule parameters M^2 , s_0^D , μ , as specified in Sect. 3, whereas at very large $|q^2|$ some of the choices have to be modified. In addition, at large virtualities, $|q^2| \gg \mu^2, m_c^2$, large logarithms in NLO terms can destroy the balance of perturbative expansion. Finally, at very large negative q^2 , the lower limit of integration u_0 in LCSR moves too close to 1, and this may potentially influence the twist expansion.

Turning to the fit procedure, we fix the $q^2 = 0$ values of the form factors (16) and (17) obtained from LCSR's and, in addition, calculate the shapes of the form factors $f_{D\pi(K)}^+(q^2)/f_{D\pi(K)}^+(0)$ at $-2 \text{ GeV}^2 < q^2 \leq 0$. The uncertainty is determined in the same way as described in Sect. 4 for the form factors at $q^2 = 0$. The calculated $D \rightarrow \pi$ and $D \rightarrow K$ form factors and their shapes at $q^2 \leq 0$ are displayed in Figs. 3 and 4, respectively. Note that the shapes have smaller uncertainties than the form factors themselves, because in the ratios some uncertainties cancel (e.g., the one due to f_D).

The calculated shapes, taking into account their uncertainties, are then fitted to the BK and series parameterizations, presented in (37) and (42), respectively. In the series parameterization (42) we choose $t_0 = t_+ - \sqrt{t_+ - t_-} \sqrt{t_+ - q_{min}^2}$, so that the whole interval $q_{min}^2 = -2 \text{ GeV}^2 < q^2 \leq t_-$ relevant for the calculation and subsequent continuation of the form factor is mapped onto the narrowest possible interval $|z| < 0.22$ ($|z| < 0.09$) for $D \rightarrow \pi$ ($D \rightarrow K$). We found that both parameterizations describe the shapes calculated at $q^2 \leq 0$ reasonably well. In addition, we also fitted the form factors to the simplest one-pole parameterization, but the fits yield an unnaturally small, lower than $m_{D(s)^*}$, pole mass. Moreover, after continuing to positive q^2 , the one-pole form factor noticeably deviates from the experimentally measured shape.

The parameters of BK parameterization $\alpha_{D\pi}$ and α_{DK} obtained from our fit are shown in Table 4, in comparison with the experimental [2] and lattice QCD [32] BK-fits. Previous LCSR estimates of these parameters [15] are smaller but have also larger errors;

Table 4: *The shape parameters of BK parametrization*

Method	Ref	$f_{D\pi}^+(q^2)$	$f_{DK}^+(q^2)$
LCSR at $q^2 \leq 0$	this work	$\alpha_{D\pi} = 0.21_{-0.07}^{+0.11}$	$\alpha_{DK} = 0.17_{-0.13}^{+0.16}$
Experiment	[2]	$\alpha_{D\pi} = 0.21 \pm 0.07 \pm 0.02$	$\alpha_{DK} = 0.30 \pm 0.03 \pm 0.01$
Lattice QCD	[32]	$\alpha_{D\pi} = 0.44 \pm 0.04 \pm 0.07$	$\alpha_{DK} = 0.50 \pm 0.04 \pm 0.07$

³In fact, this region corresponds to a hypothetical (but still physical) process of $l\pi(K) \rightarrow \nu_l D$ scattering.

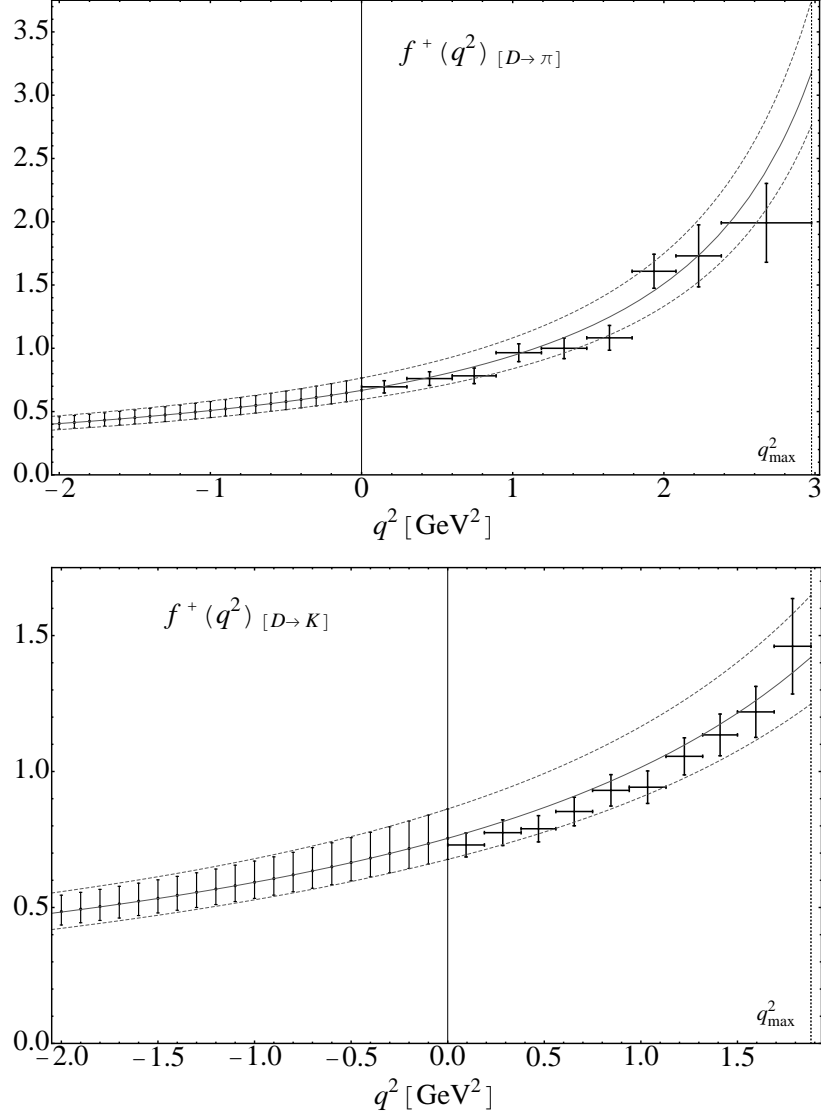


Figure 3: Form factors $f_{D\pi}^+(q^2)$ (upper panel) and $f_{DK}^+(q^2)$ (lower panel). The LCSR results with uncertainties (points with error bars at $q^2 < 0$) are fitted to series-parameterization (solid line and dashed lines indicating uncertainties) and compared to the CLEO measurements [1] (points with error bars at $q^2 > 0$), where $|V_{cd}|$ and $|V_{cs}|$ are taken from [28].

in fact, they have been determined from a different procedure, where, in addition to the LCSR form factor at $q^2 = 0$, the calculated $D^*D\pi$ coupling was used, adding its own uncertainty.

For the series parameterization (42), a fit is possible already at $N = 2$, i.e., with only

one free parameter b_1 for the shape (b_2 is fixed from the condition (40)). We obtain:

$$b_1^{D\pi} = -0.8_{-0.4}^{+0.3}, \quad b_1^{DK} = -0.9_{-0.8}^{+0.7}. \quad (43)$$

Fits at $N = 3, 4$ were also performed, yielding numerically very close results. For $N \geq 5$ the unitarity bounds [21] start to constrain the coefficients b_k .

In what follows, we choose the $N = 2$ series parameterization to be our preferred analytic expression for the shape, having in mind that it is less model-dependent than the effective pole ansatz for the dispersion integral. Continuing this parameterization to the semileptonic region $q^2 \leq t_- = (m_D - m_{\pi(K)})^2 = 2.98 \text{ GeV}^2 (1.88 \text{ GeV}^2)$, we compare in Fig. 3 the form factors with the experimentally measured ones, presented in [1] in q^2 -bins. For the normalization of the data we take the averages: $|V_{cd}| = 0.230 \pm 0.011$ and $|V_{cs}| = 1.04 \pm 0.06$ from [28]. The form factor shapes, which are independent of normalization at $q^2 = 0$ and CKM parameters, are displayed in Fig. 4. We compare our predictions for the series parameterization with the shapes obtained in [2] and observe a good agreement ⁴.

Furthermore, we calculate the total semileptonic widths divided by the square of CKM parameters from

$$\frac{\Gamma(D^0 \rightarrow \pi^- \ell^+ \nu_\ell)}{|V_{cd}|^2} = \frac{G_F^2}{24\pi^3} \int_0^{(m_D - m_\pi)^2} dq^2 \left[\left(\frac{m_D^2 + m_\pi^2 - q^2}{2m_D} \right)^2 - m_\pi^2 \right]^{\frac{3}{2}} |f_{D\pi}^+(q^2)|^2, \quad (44)$$

(at $m_l = 0$) and the analogous formula for $\Gamma(D^0 \rightarrow K^- \ell^+ \nu_\ell)/|V_{cs}|^2$, using the predicted shape of the form factors (with the series parameterization) and their normalization at $q^2 = 0$. Again, in the case of $D \rightarrow \pi$ a better accuracy is achieved by normalizing with the product $f_D f_{D\pi}^+(0)$ calculated from LCSR. To this end, multiplying both sides of (44) by f_D^2 (in the isospin limit) we replace this factor on l.h.s. by the leptonic width, using

$$\Gamma(D^+ \rightarrow \ell^+ \nu_\ell) = \frac{G_F^2}{8\pi} |V_{cd}|^2 f_D^2 m_\ell^2 m_D \left(1 - \frac{m_\ell^2}{m_D^2} \right)^2, \quad (45)$$

and obtain the following prediction:

$$\frac{\Gamma(D^0 \rightarrow \pi^- \ell^+ \nu_\ell) \Gamma(D^\pm \rightarrow \ell^\pm \nu_\ell)}{|V_{cd}|^4} = (4.7_{-0.9}^{+1.4}) \cdot 10^{-28} \text{ GeV}^2. \quad (46)$$

Employing the experimental numbers for the branching fractions from the latest CLEO measurements: $BR(D^0 \rightarrow \pi^- e^+ \nu_e) = 0.288 \pm 0.008 \pm 0.003\%$ [2], $BR(D^+ \rightarrow \mu^+ \nu_\mu) = (3.82 \pm 0.32 \pm 0.09) \times 10^{-4}$ [30], and using $\tau_{D^\pm} = (1.040 \pm 0.007) ps$, $\tau_{D^0} = (0.4101 \pm 0.0015) ps$ [28], we obtain

$$|V_{cd}| = 0.221 \pm 0.002 \pm 0.005_{-0.011}^{+0.017}, \quad (47)$$

⁴ Note that in [2] a different version of series parameterization is used to fit the shape, hence we do not directly compare the fitted parameters.

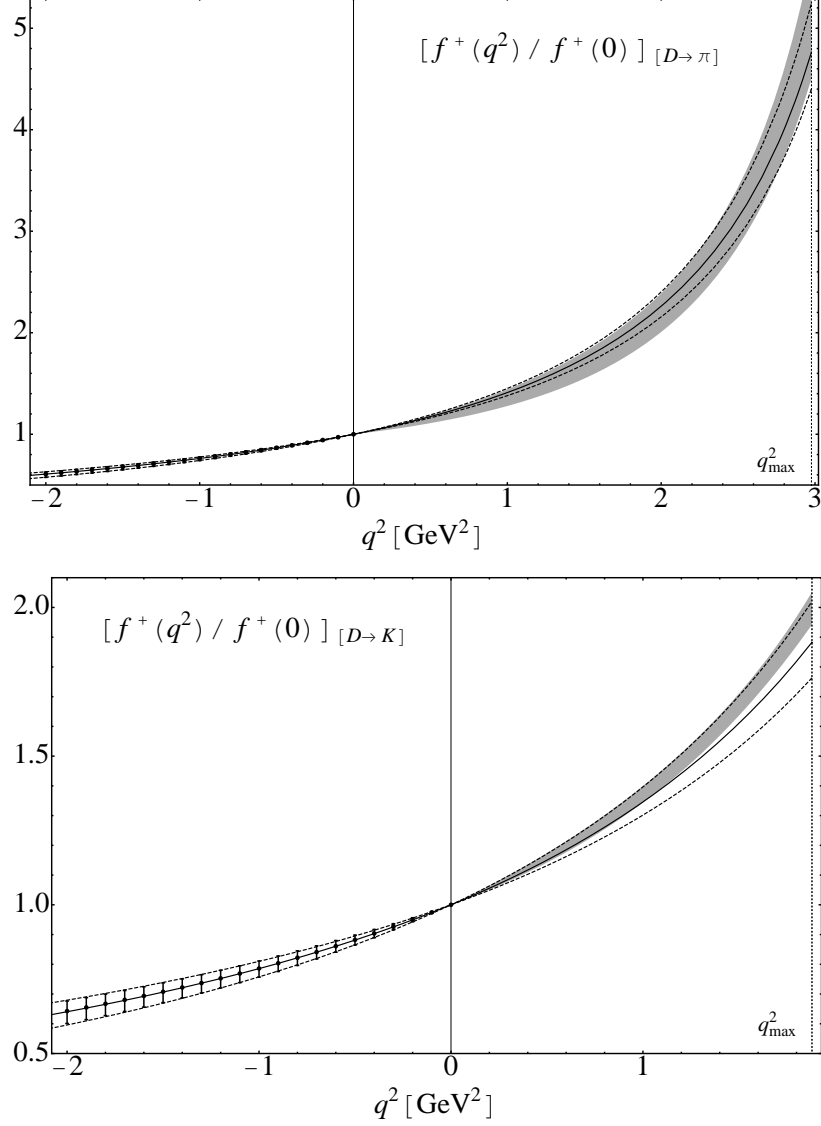


Figure 4: *The shapes of the $D \rightarrow \pi$ (upper panel) and $D \rightarrow K$ (lower panel) form factors obtained from LCSR's at negative q^2 (points with error bars), fitted to the series parameterization (solid line and dashed lines indicating uncertainties) and compared to the shapes measured by CLEO [2] (shaded regions).*

with the errors originating from the semileptonic and leptonic branching fractions and theoretical uncertainty, respectively. This determination is somewhat independent of (30) because it involves also the measured shape of $f^+(q^2)|V_{cd}|$. For the ratio of total semileptonic widths we obtain:

$$\frac{|V_{cs}|^2 \Gamma(D^0 \rightarrow \pi^- \ell^+ \nu_\ell)}{|V_{cd}|^2 \Gamma(D^0 \rightarrow K^- \ell^+ \nu_\ell)} = 1.65 \pm 0.2. \quad (48)$$

Substituting the CLEO results for the branching fractions of these channels: the one quoted above and $BR(D^0 \rightarrow K^- e^+ \nu_\ell) = 3.50 \pm 0.03 \pm 0.04\%$ [2], yields

$$\frac{|V_{cd}|}{|V_{cs}|} = 0.223 \pm 0.003 \pm 0.002 \pm 0.015. \quad (49)$$

where the errors are from semileptonic $D \rightarrow \pi$, $D \rightarrow K$ branching fractions and the LCSR result (48), respectively. To shorten this discussion, we do not present here a comparison with the data of other experiments on charm semileptonic decays [4, 5, 6], having in mind their general agreement with the CLEO data.

Concluding this section, we turn to the scalar form factor $f_{D\pi(K)}^0(q^2)$ which is obtained, substituting the LCSR results for $f_{D\pi(K)}^+(q^2)$ and $[f_{D\pi(K)}^+(q^2) + f_{D\pi(K)}^-(q^2)]$ in (2). We fit the scalar form factors calculated at negative q^2 to the series parameterization of the type (42) (without the $D_{(s)}^*$ -pole factor which is irrelevant in this case). The results for $N = 2$ are

$$b_1^{f^0, D\pi} = -2.6_{-0.5}^{+0.3}, \quad b_1^{f^0, DK} = -3.3_{-0.8}^{+0.6}. \quad (50)$$

Going to $N \geq 3$ demands dedicated unitarity bounds in the scalar heavy-light channel which, to our knowledge have not been derived and are beyond our scope.

The predicted scalar form factors are plotted in Fig. 5.

Our results are in agreement with $f_{D\pi}^0$ and f_{DK}^0 presented in [32] in a form of BK parameterization

$$f_{D\pi(K)}^0(q^2) = \frac{1}{1 - q^2/(\beta_{D\pi(K)} m_{D_{(s)}^*}^2)}, \quad (51)$$

with $\beta_{D\pi} = 1.41 \pm 0.06 \pm 0.07$, $\beta_{DK} = 1.31 \pm 0.07 \pm 0.13$. Our fit to (51) yields: $\beta_{D\pi} = 1.25 \pm 0.2$, $\beta_{DK} = 1.3_{-0.3}^{+0.4}$, with larger uncertainties.

Finally, we extrapolate the scalar form factors to the unphysical point $q^2 = m_D^2$, located slightly above t_- , and obtain

$$f_{D\pi}^0(m_D^2) = 1.40_{-0.14}^{+0.21}, \quad f_{DK}^0(m_D^2) = 1.29_{-0.16}^{+0.23}. \quad (52)$$

These results can be compared to the approximate relation

$$\lim_{q^2 \rightarrow m_D^2} f_{D\pi(K)}^0(q^2) = f_D/f_{\pi(K)} = 1.58 \pm 0.07 \quad (1.32 \pm 0.06), \quad (53)$$

derived from the current algebra combined with the soft pion (kaon) limit [39], where we used the measured values [28, 30] of the decay constants.

7. Summary

In this paper we returned to the calculation of $D \rightarrow \pi$ and $D \rightarrow K$ form factors from LCSR's. Several improvements have been implemented, including the use of \overline{MS} c -quark mass, and updated parameters of pion and kaon DA's.

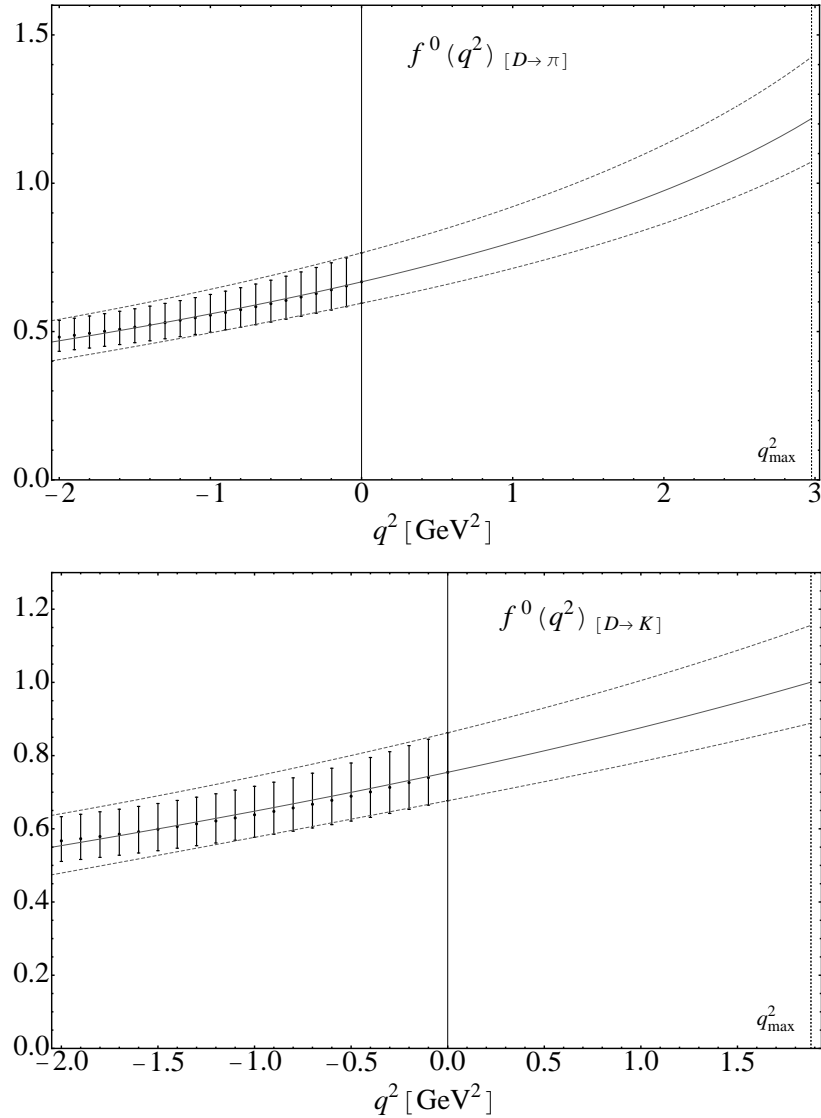


Figure 5: Scalar form factors $f_{D\pi(K)}^0$ obtained from fitting the LCSR result at negative q^2 to the series parameterization. Notations the same as in Fig. 3.

The main advancement is in the phenomenological direction. Employing the accurate measurement of the D -meson decay constant, we effectively decreased the theoretical uncertainty of $|V_{cd}|$ determination from the $D \rightarrow \pi l \nu_l$ decay distribution, using the LCSR prediction for the product of the $D \rightarrow \pi$ form factor and f_D . The uncertainty in the determination of $|V_{cs}|$ is also reduced, due to a better knowledge of the s -quark mass and various $SU(3)_{fl}$ violating effects in the kaon DA's. Our results for $|V_{cd}|$ and $|V_{cs}|$ are in agreement with lattice QCD determinations.

A new element presented in this paper is the prediction of the $D \rightarrow \pi, K$ form factors

in the whole semileptonic region, combining LCSR calculation with the analyticity of the form factors. The latter property is cast in the form of conformal mapping and series parameterization, in the version recently suggested in [21]. The form factor shapes obtained from this combined procedure are in a good agreement with the latest experimental measurements of the semileptonic charm decay distributions by CLEO collaboration. Our analysis based on the conformal mapping can be further refined, by using more terms in the power series and implementing the constraints from the dedicated unitarity bounds. Applications to other hadronic form factors calculated from LCSR are also possible.

Another interesting task which will be studied elsewhere, is the comparison of $B \rightarrow \pi$ and $D \rightarrow \pi$ form factors, calculated at two different finite quark masses, with the combined heavy-quark mass and large recoil limit. Such a comparison will allow one to quantify the deviations from the symmetry relations in this limit, as well as the proportion of hard-scattering and soft-overlap mechanisms in the heavy-light form factors.

LCSR's provide analytical, but essentially approximate expressions for the hadronic form factors. The accuracy of light-cone OPE is limited, due to finite amount of terms in the twist expansion and uncertainties in the parameters of pion and kaon DA's. A further improvement of OPE is possible, e.g., if the subleading twist-5 terms are calculated. For that one needs a separate study of pion and kaon twist-5 DA's. The gluon radiative corrections to the subleading twist-4 and three-particle terms represent a technically difficult task, but we expect these corrections to be very small. A further limitation of the accuracy is caused by the quark-hadron duality approximation used to model the hadronic spectral density in LCSR. The resulting uncertainty is difficult to estimate, still it is effectively minimized in the sum rules.

The comparison of our predictions for charm semileptonic decays with experiment and lattice QCD ensures optimism and provides an additional test for the important applications of the LCSR method, such as the $|V_{ub}|$ determination from exclusive semileptonic $B \rightarrow \pi$ decays.

Acknowledgements

This work is supported by the Deutsche Forschungsgemeinschaft under the contract No. KH205/1-2. Work of N.O. is supported by EU Contract No.MRTN-CT-2006-035482, "FLAVIANet". A.K. also acknowledges the travel support of "FLAVIANet" during his visit to Orsay.

Appendix

A. Summary of the K -meson distribution amplitudes

Here we present the definitions and the expressions of the two- and three-particle K -meson DA's of twist 2,3 and 4 used in LCSR. The corresponding formulae for pion DA's are obtained by replacing everywhere $K \rightarrow \pi$, $s \rightarrow d$, $m_K \rightarrow m_\pi$, $m_s \rightarrow m_d \rightarrow 0$ and $\mu_K \rightarrow \mu_\pi$.

A.1. Definitions

The K -meson two-particle DA's are defined from the following bilocal matrix element:

$$\begin{aligned} \langle K^-(p) | \bar{s}_\omega^i(x_1) u_\xi^j(x_2) | 0 \rangle_{x^2 \rightarrow 0} &= \frac{i\delta^{ij}}{12} f_K \int_0^1 du e^{iup \cdot x_1 + i\bar{u}p \cdot x_2} \left([\not{p}\gamma_5]_{\xi\omega} \varphi_K(u) \right. \\ &\quad - [\gamma_5]_{\xi\omega} \mu_K \phi_{3K}^p(u) + \frac{1}{6} [\sigma_{\beta\tau}\gamma_5]_{\xi\omega} p_\beta(x_1 - x_2)_\tau \mu_K \phi_{3K}^\sigma(u) \\ &\quad \left. + \frac{1}{16} [\not{p}\gamma_5]_{\xi\omega} (x_1 - x_2)^2 \phi_{4K}(u) - \frac{i}{2} [(\not{x}_1 - \not{x}_2)\gamma_5]_{\xi\omega} \int_0^u \psi_{4K}(v) dv \right), \end{aligned} \quad (54)$$

where the variable u ($\bar{u} = 1 - u$) is the fraction of the meson momentum carried by the s -quark (light antiquark). This decomposition contains the twist-2 DA $\varphi_K(u)$, twist-3 DA's $\phi_{3K}^p(u)$ and $\phi_{3K}^\sigma(u)$, and twist-4 DA's $\phi_{4K}(u)$ and $\psi_{4K}(u)$. The definition of each separate DA is easily obtained, multiplying both parts of the above equation by the corresponding combinations of γ matrices and taking Dirac and color traces.

In the same way, the three-particle DA's are defined via the matrix element:

$$\begin{aligned} \langle K^-(p) | \bar{s}_\omega^i(x_1) g_s G_{\mu\nu}^a(x_3) u_\xi^j(x_2) | 0 \rangle_{x^2 \rightarrow 0} &= \frac{\lambda_{ji}^a}{32} \int \mathcal{D}\alpha_i e^{ip(\alpha_1 x_1 + \alpha_2 x_2 + \alpha_3 x_3)} \\ &\times \left[i f_{3K} (\sigma_{\lambda\rho}\gamma_5)_{\xi\omega} (p_\mu p_\lambda g_{\nu\rho} - p_\nu p_\lambda g_{\mu\rho}) \Phi_{3K}(\alpha_i) \right. \\ &\quad - f_K (\gamma_\lambda \gamma_5)_{\xi\omega} \left\{ (p_\nu g_{\mu\lambda} - p_\mu g_{\nu\lambda}) \Psi_{4K}(\alpha_i) + \frac{p_\lambda (p_\mu x_\nu - p_\nu x_\mu)}{(p \cdot x)} (\Phi_{4K}(\alpha_i) + \Psi_{4K}(\alpha_i)) \right\} \\ &\quad \left. - \frac{i f_K}{2} \epsilon_{\mu\nu\delta\rho} (\gamma_\lambda)_{\xi\omega} \left\{ (p^\rho g^{\delta\lambda} - p^\delta g^{\rho\lambda}) \tilde{\Psi}_{4K}(\alpha_i) + \frac{p_\lambda (p^\delta x^\rho - p^\rho x^\delta)}{(p \cdot x)} (\tilde{\Phi}_{4K}(\alpha_i) + \tilde{\Psi}_{4K}(\alpha_i)) \right\} \right]. \end{aligned} \quad (55)$$

where $\Phi_{3K}(\alpha_i)$ is of twist-3 and the other four DA's are of twist-4.

In addition, in [19] one more three-particle twist-4 DA $\Xi_{4K}(\alpha_i)$ is taken into consideration, originating from the operator which contains a covariant derivative of the gluon field:

$$\langle K(p) | \bar{s}(x_1) \gamma_\mu \gamma_5 g D^\alpha G_{\alpha\beta}(x_3) q(x_2) | 0 \rangle = -i f_K p_\mu p_\beta \int \mathcal{D}\alpha_i e^{ip(\alpha_1 x_1 + \alpha_2 x_2 + \alpha_3 x_3)} \Xi_{4K}(\alpha_i). \quad (56)$$

The three-particle DA's depend on momentum fraction variables $\alpha_i = \{\alpha_1, \alpha_2, \alpha_3\}$ and the integration measure is $\mathcal{D}\alpha_i = d\alpha_1 d\alpha_2 d\alpha_3 \delta(1 - \alpha_1 - \alpha_2 - \alpha_3)$.

For the total antisymmetric tensor we use the convention $\epsilon^{0123} = -1$, which corresponds to $Tr\{\gamma^5 \gamma^\mu \gamma^\nu \gamma^\alpha \gamma^\beta\} = 4i\epsilon^{\mu\nu\alpha\beta}$.

In the following, we list the expressions for all DA's entering (54), (55) and (56), based on NLO in conformal expansion and operator identities and updated in [19].

A.2. Twist-2 distribution amplitudes

The twist-2 $\varphi_K(u)$ distribution amplitude is expanded in a series of Gegenbauer polynomials:

$$\varphi_K(u, \mu) = 6u(1-u) \left(1 + \sum_{n=1,2,\dots} a_n^K(\mu) C_n^{3/2}(2u-1) \right), \quad (57)$$

where only the first two coefficients (Gegenbauer moments) $a_1^K(\mu)$ and $a_2^K(\mu)$ are retained and LO scale-dependence is taken into account. The formulae for the scale-dependence of these and other relevant DA parameters can be found, e.g., in [19].

A.3. Twist-3 distribution amplitudes

In the same approximation, the twist-3 DA's are described by μ_K and three additional parameters $f_{3K}, \omega_{3K}, \lambda_{3K}$. Their definitions in terms of hadronic matrix elements of local operators are given in [19]. We also use the short-hand notation

$$\eta_{3K} = \frac{f_{3K}}{f_K \mu_K}.$$

In our calculation we neglect the u, d quark masses, hence the expressions presented here are somewhat simpler than the original ones in [19]. In particular, in the adopted approximation the parameters ρ_+^K, ρ_-^K introduced in [19] are equal:

$$\rho_+^K = \rho_-^K \equiv \rho^K = \frac{m_s}{\mu_K}. \quad (58)$$

The twist-3 kaon DA's used in our calculation are:

$$\begin{aligned} \phi_{3K}^p(u) &= 1 + 3\rho^K(1 - 3a_1^K + 6a_2^K)(1 + \ln u) \\ &\quad - \frac{\rho^K}{2}(3 - 27a_1^K + 54a_2^K)C_1^{1/2}(2u-1) \\ &\quad + 3\left(10\eta_{3K} - \rho^K(a_1^K - 5a_2^K)\right)C_2^{1/2}(2u-1) \\ &\quad + \left(10\eta_{3K}\lambda_{3K} - \frac{9}{2}\rho^K a_2^K\right)C_3^{1/2}(2u-1) - 3\eta_{3K}\omega_{3K}C_4^{1/2}(2u-1), \end{aligned} \quad (59)$$

$$\begin{aligned}
\phi_{3K}^\sigma(u) &= 6u\bar{u} \left\{ 1 + \frac{\rho^K}{2} (3 - 15a_1^K + 30a_2^K) \right. \\
&+ \rho^K \left(3a_1^K - \frac{15}{2}a_2^K \right) C_1^{3/2} (2u - 1) \\
&+ \frac{1}{2} \left(\eta_{3K} (10 - \omega_{3K}) + 3\rho^K a_2^K \right) C_2^{3/2} (2u - 1) + \eta_{3K} \lambda_{3K} C_3^{3/2} (2u - 1) \\
&\left. + 3\rho^K (1 - 3a_1^K + 6a_2^K) \ln u \right\}, \tag{60}
\end{aligned}$$

$$\Phi_{3K}(\alpha_i) = 360\alpha_1\alpha_2\alpha_3^2 \left\{ 1 + \lambda_{3K}(\alpha_1 - \alpha_2) + \omega_{3K} \frac{1}{2} (7\alpha_3 - 3) \right\}. \tag{61}$$

A.4. Twist-4 distribution amplitudes

As explained in detail in [19], the twist-4 DA's are described by 13 parameters of the conformal expansion. They are expressed via three nonperturbative parameters $\delta_K^2, \omega_{4K}, \kappa_{4K}$ and in addition fixed by the renormalon model of twist-4 DA's. Here we give the expressions for the twist-4 kaon DA's, where the above mentioned relations are already substituted and the same approximation as for twist-3 DA's is adopted.

We rederived the expressions (4.27) and (4.28) in [19] for the twist-4 two-particle DA's defined in (4.26) and using the operator relations given there in (A1),(A2). We found that both (4.27) and (4.28) should be corrected by replacing $\psi_{4;K}(u) \rightarrow \psi_{4;K}(u) + m_K^2 \phi_{2;K}$ (in the notations of [19]). In fact, our version of $\psi_{4;K}(u)$ agrees with the function $B(u)$ introduced in [40]. Moreover, we restore the correct normalization $\int_0^1 \psi_{4;K}(u) du = 0$.

We use the following expressions for two-particle twist-4 DA's:

$$\psi_{4K}(u) = \psi_{4K}^{T4}(u) + \psi_{4K}^{WW}(u), \tag{62}$$

where

$$\psi_{4K}^{T4}(u) = \delta_K^2 \left\{ \frac{20}{3} C_2^{1/2} (2u - 1) + \frac{49}{2} a_1^K C_3^{1/2} (2u - 1) \right\}, \tag{63}$$

and (the corrected version)

$$\begin{aligned}
\psi_{4K}^{WW}(u) &= m_K^2 \left\{ \left[6\rho^K (1 - 3a_1^K + 6a_2^K) \right] C_0^{1/2} (2u - 1) \right. \\
&- \left[\frac{18}{5} a_1^K + 3\rho^K (1 - 9a_1^K + 18a_2^K) + 12\kappa_{4K} \right] C_1^{1/2} (2u - 1) \\
&+ \left[2 - 6\rho^K (a_1^K - 5a_2^K) + 60\eta_{3K} \right] C_2^{1/2} (2u - 1) \\
&+ \left[\frac{18}{5} a_1^K - 9\rho^K a_2^K + \frac{16}{3} \kappa_{4K} + 20\eta_{3K} \lambda_{3K} \right] C_3^{1/2} (2u - 1) \\
&\left. + \left[\frac{9}{4} a_2^K - 6\eta_{3K} \omega_{3K} \right] C_4^{1/2} (2u - 1) \right\} + 6m_s^2 (1 - 3a_1^K + 6a_2^K) \ln u, \tag{64}
\end{aligned}$$

Table 5: Parameters of the pion and kaon DA's (normalized at 1 GeV): a_2^π, a_4^π are fitted in [13], a_1^K from [18], all others from [19]. κ_4^K is calculated from (73).

a_1^π	0	a_1^K	0.10 ± 0.04
a_2^π	0.16 ± 0.01	a_2^K	0.25 ± 0.15
a_4^π	0.04 ± 0.01	a_4^K	0
$a_{>4}^\pi$	0	$a_{>4}^K$	0
f_3^π	$(0.0045 \pm 0.0015) \text{ GeV}^2$	f_3^K	$(0.0045 \pm 0.0015) \text{ GeV}^2$
ω_3^π	-1.5 ± 0.7	ω_3^K	-1.2 ± 0.7
λ_3^π	0	λ_3^K	1.6 ± 0.4
ω_4^π	0.2 ± 0.1	ω_4^K	0.2 ± 0.1
δ_π^2	$(0.18 \pm 0.06) \text{ GeV}^2$	δ_K^2	$(0.2 \pm 0.06) \text{ GeV}^2$
$\kappa_{4\pi}$	0	κ_{4K}	-0.12 ± 0.01

$$\phi_{4K}(u) = \phi_{4K}^{T4}(u) + \phi_{4K}^{WW}(u), \quad (65)$$

where

$$\begin{aligned} \phi_{4K}^{T4}(u) = & \delta_K^2 \left\{ \left(\frac{200}{3} + 196(2u-1)a_1^K \right) u^2 \bar{u}^2 \right. \\ & + 21\omega_{4K} \left(u\bar{u}(2+13u\bar{u}) + [2u^3(6u^2-15u+10)\ln u] + [u \leftrightarrow \bar{u}] \right) \\ & \left. - 14a_1^K \left(u\bar{u}(2u-1)(2-3u\bar{u}) - [2u^3(u-2)\ln u] + [u \leftrightarrow \bar{u}] \right) \right\}, \quad (66) \end{aligned}$$

$$\begin{aligned} \phi_{4K}^{WW}(u) = & m_K^2 \left\{ \frac{16}{3}\kappa_{4K} \left(u\bar{u}(2u-1)(1-2u\bar{u}) + [5(u-2)u^3\ln u] - [u \leftrightarrow \bar{u}] \right) \right. \\ & + 4\eta_{3K}u\bar{u} \left(60\bar{u} + 10\lambda_{3K}[(2u-1)(1-u\bar{u}) - (1-5u\bar{u})] \right) \\ & - \omega_{3K} [3 - 21u\bar{u} + 28u^2\bar{u}^2 + 3(2u-1)(1-7u\bar{u})] \\ & - \frac{36}{5}a_2^K \left(\frac{1}{4}u\bar{u}(4-9u\bar{u}+110u^2\bar{u}^2) + [u^3(10-15u+6u^2)\ln u] + [u \leftrightarrow \bar{u}] \right) \\ & \left. + 4u\bar{u}(1+3u\bar{u}) \left(1 + \frac{9}{5}(2u-1)a_1^K \right) \right\}. \quad (67) \end{aligned}$$

The twist-4 three-particle DAs have the following expressions:

$$\begin{aligned} \Phi_{4K}(\alpha_i) = & 120\alpha_1\alpha_2\alpha_3 \left\{ \delta_K^2 \left[\frac{21}{8}(\alpha_1 - \alpha_2)\omega_{4K} + \frac{7}{20}a_1^K(1-3\alpha_3) \right] \right. \\ & \left. + m_K^2 \left[-\frac{9}{20}(\alpha_1 - \alpha_2)a_2^K + \frac{1}{3}\kappa_{4K} \right] \right\}, \quad (68) \end{aligned}$$

$$\tilde{\Phi}_{4K}(\alpha_i) = -120\alpha_1\alpha_2\alpha_3\delta_K^2\left\{\frac{1}{3} + \frac{7}{4}a_1^K(\alpha_1 - \alpha_2) + \frac{21}{8}\omega_{4K}(1 - 3\alpha_3)\right\}, \quad (69)$$

$$\begin{aligned} \Psi_{4K}(\alpha_i) &= 30\alpha_3^2\left\{\delta_K^2\left[\frac{1}{3}(\alpha_1 - \alpha_2) + \frac{7}{10}a_1^K[-\alpha_3(1 - \alpha_3) + 3(\alpha_1 - \alpha_2)^2]\right.\right. \\ &\quad \left.+\frac{21}{4}\omega_{4K}(\alpha_1 - \alpha_2)(1 - 2\alpha_3)\right] \\ &\quad \left.+m_K^2(1 - \alpha_3)\left[\frac{9}{40}(\alpha_1 - \alpha_2) - \frac{1}{3}\kappa_{4K}\right]\right\}, \end{aligned} \quad (70)$$

$$\begin{aligned} \tilde{\Psi}_{4K}(\alpha_i) &= 30\alpha_3^2\left\{\delta_K^2\left[\frac{1}{3}(1 - \alpha_3) - \frac{7}{10}a_1^K(\alpha_1 - \alpha_2)(4\alpha_3 - 3)\right.\right. \\ &\quad \left.+\frac{21}{4}\omega_{4K}(1 - \alpha_3)(1 - 2\alpha_3)\right] \\ &\quad \left.+m_K^2\left[\frac{9}{40}a_2^K(\alpha_1^2 - 4\alpha_1\alpha_2 + \alpha_2^2) - \frac{1}{3}(\alpha_1 - \alpha_2)\kappa_{4K}\right]\right\}, \end{aligned} \quad (71)$$

$$\Xi_{4K}(\alpha_i) = 840\alpha_1\alpha_2\alpha_3^3\Xi_0^K, \quad (72)$$

Using the equations of motion, the parameter κ_{4K} can be expressed via a_1^K and the quark mass:

$$\kappa_{4K} = -\frac{1}{8} - \frac{9}{40}a_1^K + \frac{m_s}{2\mu_K}, \quad (73)$$

and the parameter entering Ξ_{4K} is taken from the renormalon model [19]:

$$\Xi_0^K = \frac{1}{5}\delta_K^2 a_1^K \quad (74)$$

The numerical values for all parameters entering the pion- and kaon- DA's are collected in Table 5.

B. Contributions to LCSR

Here we present the separate contributions to LCSR's for the form factors f_{DK}^+ and $(f_{DK}^+ + f_{DK}^-)$ including LO twist-2,-3 and -4 terms. The corresponding contributions for $D \rightarrow \pi$ form factors are obtained by replacing: the kaon DA's by the pion DA's, $m_K \rightarrow m_\pi \simeq 0$ and $m_s \rightarrow m_d \simeq 0$.

$$F_0^{K,2}(q^2, M^2, s_0^D) = m_c^2 f_K \int_{u_0}^1 \frac{du}{u} e^{-\frac{m_c^2 - q^2 \bar{u} + m_K^2 u \bar{u}}{uM^2}} \varphi_K(u), \quad (75)$$

$$\begin{aligned}
F_0^{K,3}(q^2, M^2, s_0^D) &= m_c^2 f_K \int_{u_0}^1 du e^{-\frac{m_c^2 - q^2 \bar{u} + m_K^2 u \bar{u}}{u M^2}} \left\{ \frac{\mu_K}{m_c} \left[\phi_{3K}^p(u) \right. \right. \\
&+ \frac{1}{3} \left(\frac{1}{u} - \frac{m_c^2 + q^2 - u^2 m_K^2}{2(m_c^2 - q^2 + u^2 m_K^2)} \frac{d}{du} - \frac{2um_K^2 m_c^2}{(m_c^2 - q^2 + u^2 m_K^2)^2} \right) \phi_{3K}^\sigma(u) \left. \right] \\
&- \frac{f_{3K}}{m_c f_K} \left[\frac{2}{u} \left(\frac{m_c^2 - q^2 - u^2 m_K^2}{m_c^2 - q^2 + u^2 m_K^2} \right) \left(\frac{d}{du} - \frac{2um_K^2}{m_c^2 - q^2 + u^2 m_K^2} \right) I_{3K}(u) \right. \\
&\left. \left. + \frac{3m_K^2}{m_c^2 - q^2 + u^2 m_K^2} \left(\frac{d}{du} - \frac{2um_K^2}{m_c^2 - q^2 + u^2 m_K^2} \right) \bar{I}_{3K}(u) \right] \right\}, \tag{76}
\end{aligned}$$

$$\begin{aligned}
F_0^{K,4}(q^2, M^2, s_0^D) &= m_c^2 f_K \int_{u_0}^1 du e^{-\frac{m_c^2 - q^2 \bar{u} + m_K^2 u \bar{u}}{u M^2}} \left\{ \right. \\
&\frac{1}{m_c^2 - q^2 + u^2 m_K^2} \left[u \psi_{4K}(u) + \left(1 - \frac{2u^2 m_K^2}{m_c^2 - q^2 + u^2 m_K^2} \right) \int_0^u dv \psi_{4K}(v) \right. \\
&- \frac{m_c^2 u}{4(m_c^2 - q^2 + u^2 m_K^2)} \left(\frac{d^2}{du^2} - \frac{6um_K^2}{m_c^2 - q^2 + u^2 m_K^2} \frac{d}{du} + \frac{12um_K^4}{(m_c^2 - q^2 + u^2 m_K^2)^2} \right) \phi_{4K}(u) \\
&- \left(\frac{d}{du} - \frac{2um_K^2}{m_c^2 - q^2 + u^2 m_K^2} \right) \left(I_{4K}(u) - \frac{dI_{4K}^\Xi(u)}{du} \right) \\
&- \frac{2um_K^2}{m_c^2 - q^2 + u^2 m_K^2} \left(u \frac{d}{du} + \left(1 - \frac{4u^2 m_K^2}{m_c^2 - q^2 + u^2 m_K^2} \right) \right) \bar{I}_{4K}(u) \\
&\left. \left. + \frac{2um_K^2(m_c^2 - q^2 - u^2 m_K^2)}{(m_c^2 - q^2 + u^2 m_K^2)^2} \left(\frac{d}{du} - \frac{6um_K^2}{m_c^2 - q^2 + u^2 m_K^2} \right) \int_u^1 d\xi \bar{I}_{4K}(\xi) \right] \right\} \\
&+ \frac{m_c^4 f_K e^{-\frac{m_c^2}{M^2}}}{4(m_c^2 - q^2 + m_K^2)^2} \left(\frac{d\phi_{4K}^{WW}(u)}{du} \right)_{u \rightarrow 1}, \tag{77}
\end{aligned}$$

where $\bar{u} = 1 - u$, $u_0 = \left(q^2 - s_0^D + m_K^2 + \sqrt{(s_0^D - q^2 - m_K^2)^2 + 4m_K^2(m_c^2 - q^2)} \right) / (2m_K^2)$, and the short-hand notations introduced for the integrals over three-particle DA's are:

$$I_{3K}(u) = \int_0^u d\alpha_1 \int_{(u-\alpha_1)/(1-\alpha_1)}^1 dv \Phi_{3K}(\alpha_i) \Big|_{\substack{\alpha_2 = 1 - \alpha_1 - \alpha_3, \\ \alpha_3 = (u - \alpha_1)/v}}, \tag{78}$$

$$\bar{I}_{3K}(u) = u \int_0^u d\alpha_1 \int_{(u-\alpha_1)/(1-\alpha_1)}^1 \frac{dv}{v} (2v-1) \Phi_{3K}(\alpha_i) \Big|_{\substack{\alpha_2 = 1 - \alpha_1 - \alpha_3, \\ \alpha_3 = (u - \alpha_1)/v}}, \quad (79)$$

$$I_{4K}(u) = \int_0^u d\alpha_1 \int_{(u-\alpha_1)/(1-\alpha_1)}^1 \frac{dv}{v} \left[2\Psi_{4K}(\alpha_i) - \Phi_{4K}(\alpha_i) + 2\tilde{\Psi}_{4K}(\alpha_i) - \tilde{\Phi}_{4K}(\alpha_i) \right] \Big|_{\substack{\alpha_2 = 1 - \alpha_1 - \alpha_3, \\ \alpha_3 = (u - \alpha_1)/v}}, \quad (80)$$

$$\bar{I}_{4K}(u) = \int_0^u d\alpha_1 \int_{(u-\alpha_1)/(1-\alpha_1)}^1 \frac{dv}{v} \left[\Psi_{4K}(\alpha_i) + \Phi_{4K}(\alpha_i) + \tilde{\Psi}_{4K}(\alpha_i) + \tilde{\Phi}_{4K}(\alpha_i) \right] \Big|_{\substack{\alpha_2 = 1 - \alpha_1 - \alpha_3, \\ \alpha_3 = (u - \alpha_1)/v}}, \quad (81)$$

$$I_{4K}^{\Xi}(u) = \int_0^u d\alpha_1 \int_{(u-\alpha_1)/(1-\alpha_1)}^1 \frac{dv}{v} \left[v(1-v)\Xi_{4K}(\alpha_i) \right] \Big|_{\substack{\alpha_2 = 1 - \alpha_1 - \alpha_3, \\ \alpha_3 = (u - \alpha_1)/v}}. \quad (82)$$

The LCSR for $(f_{DK}^+ + f_{DK}^-)$ in LO has the following contributions:

$$\tilde{F}_0^{K,2}(q^2, M^2, m_c^2, s_0^D) = 0, \quad (83)$$

$$\begin{aligned} \tilde{F}_0^{K,3}(q^2, M^2, s_0^D) &= m_c^2 f_K \int_{u_0}^1 du e^{-\frac{m_c^2 - q^2 \bar{u} + m_K^2 u \bar{u}}{uM^2}} \left\{ \frac{\mu_K}{m_c} \left(\frac{\phi_{3K}^p(u)}{u} + \frac{1}{6u} \frac{d\phi_{3K}^\sigma(u)}{du} \right) \right. \\ &\quad \left. + \left(\frac{f_{3K}}{f_K m_c} \right) \frac{m_K^2}{m_c^2 - q^2 + u^2 m_K^2} \left(\frac{d}{du} - \frac{2um_K^2}{m_c^2 - q^2 + u^2 m_K^2} \right) \tilde{I}_{3K}(u) \right\}, \quad (84) \end{aligned}$$

where

$$\tilde{I}_{3K}(u) = \int_0^u d\alpha_1 \int_{(u-\alpha_1)/(1-\alpha_1)}^1 \frac{dv}{v} [(3-2v)] \Phi_{3K}(\alpha_i) \Big|_{\substack{\alpha_2 = 1 - \alpha_1 - \alpha_3, \\ \alpha_3 = (u - \alpha_1)/v}}, \quad (85)$$

and

$$\begin{aligned}
\tilde{F}_0^{K,4}(q^2, M^2, s_0^D) = m_c^2 f_K \int_{u_0}^1 du e^{-\frac{m_c^2 - q^2 \bar{u} + m_K^2 u \bar{u}}{u M^2}} & \left\{ \frac{1}{m_c^2 - q^2 + u^2 m_K^2} \left[\psi_{4K}(u) \right. \right. \\
& - \frac{2um_K^2}{m_c^2 - q^2 + u^2 m_K^2} \int_0^u dv \psi_{4K}(v) + \frac{2um_K^2}{m_c^2 - q^2 + u^2 m_K^2} \left(\frac{d^2}{du^2} \right. \\
& \left. \left. - \frac{6um_K^2}{m_c^2 - q^2 + u^2 m_K^2} \frac{d}{du} + \frac{12u^2 m_K^4}{(m_c^2 - q^2 + u^2 m_K^2)^2} \right) \int_u^1 d\xi \bar{T}_{4K}(\xi) \right] \left. \right\}. \quad (86)
\end{aligned}$$

References

- [1] J. Y. Ge *et al.* [CLEO Collaboration], arXiv:0810.3878 [hep-ex].
- [2] D. Besson [CLEO Collaboration], arXiv:0906.2983 [hep-ex].
- [3] G. S. Huang *et al.* [CLEO Collaboration], Phys. Rev. Lett. **94** (2005) 011802; D. Cronin-Hennessy *et al.* [CLEO Collaboration], Phys. Rev. Lett. **100**, 251802 (2008); S. Dobbs *et al.* [CLEO Collaboration], Phys. Rev. D **77**, 112005, (2008).
- [4] J. M. Link *et al.* [FOCUS Collaboration], Phys. Lett. B **607**, 51 (2005); Phys. Lett. B **607**, 233 (2005).
- [5] L. Widhalm *et al.*, Phys. Rev. Lett. **97** (2006) 061804.
- [6] B. Aubert *et al.* [BABAR Collaboration], Phys. Rev. D **76** (2007) 052005.
- [7] I. I. Balitsky, V. M. Braun and A. V. Kolesnichenko, Nucl. Phys. **B312** (1989) 509; V. M. Braun and I. E. Filyanov, Z. Phys. **C44** (1989) 157; V. L. Chernyak and I. R. Zhitnitsky, Nucl. Phys. **B345** (1990) 137.
- [8] V. M. Belyaev, A. Khodjamirian and R. Rückl, Z. Phys. C **60** (1993) 349.
- [9] V. M. Belyaev, V. M. Braun, A. Khodjamirian and R. Rückl, Phys. Rev. D **51** (1995) 6177.
- [10] A. Khodjamirian, R. Rückl, S. Weinzierl and O. I. Yakovlev, Phys. Lett. B **410** (1997) 275.
- [11] E. Bagan, P. Ball and V. M. Braun, Phys. Lett. B **417**, 154 (1998).
- [12] P. Ball and R. Zwicky, Phys. Rev. D **71** (2005) 014015.
- [13] G. Duplancic, A. Khodjamirian, T. Mannel, B. Melic and N. Offen, JHEP **0804**, 014 (2008).
- [14] P. Ball, V. M. Braun and H. G. Dosch, Phys. Rev. D **44** (1991) 3567.

- [15] A. Khodjamirian, R. Ruckl, S. Weinzierl, C. W. Winhart and O. I. Yakovlev, Phys. Rev. D **62** (2000) 114002.
- [16] P. Ball, Phys. Lett. B **641** (2006) 50.
- [17] J. H. Kuhn, M. Steinhauser and C. Sturm, Nucl. Phys. B **778** (2007) 192;
R. Boughezal, M. Czakon and T. Schutzmeier, Phys. Rev. D **74**, 074006 (2006).
- [18] K. G. Chetyrkin, A. Khodjamirian and A. A. Pivovarov, Phys. Lett. B **661** (2008) 250.
- [19] P. Ball, V. M. Braun and A. Lenz, JHEP **0708** (2007) 090.
- [20] D. Becirevic and A. B. Kaidalov, Phys. Lett. B **478** (2000) 417.
- [21] C. Bourrely, I. Caprini and L. Lellouch, Phys. Rev. D **79** (2009) 013008.
- [22] G. Duplancic and B. Melic, Phys. Rev. D **78**, 054015 (2008).
- [23] A. Khodjamirian, R. Ruckl and C. W. Winhart, Phys. Rev. D **58** (1998) 054013.
- [24] P. Ball, arXiv:hep-ph/0308249.
- [25] I. Allison *et al.* [HPQCD Collaboration], Phys. Rev. D **78** (2008) 054513.
- [26] K. G. Chetyrkin and A. Khodjamirian, Eur. Phys. J. C **46** (2006) 721;
M. Jamin, J. A. Oller and A. Pich, Phys. Rev. D **74** (2006) 074009.
- [27] H. Leutwyler, Phys. Lett. B **378**, 313 (1996).
- [28] C. Amsler *et al.* [Particle Data Group], Phys. Lett. B **667**, 1 (2008).
- [29] A. Khodjamirian, T. Mannel and M. Melcher, Phys. Rev. D **70**, 094002 (2004).
- [30] B. I. Eisenstein *et al.* [CLEO Collaboration], Phys. Rev. D **78**, 052003 (2008).
- [31] A. Abada, D. Becirevic, P. Boucaud, J. P. Leroy, V. Lubicz and F. Mescia, Nucl. Phys. B **619**, 565 (2001).
- [32] C. Aubin *et al.* [Fermilab Lattice Collaboration, MILC Collaboration and HPQCD Collaboration], Phys. Rev. Lett. **94**, 011601 (2005);
C. Bernard *et al.*, arXiv:0906.2498 [hep-lat].
- [33] A. Al-Haydari *et al.* [QCDSF Collaboration], arXiv:0903.1664 [hep-lat].
- [34] R. J. Hill, Phys. Rev. D **73** (2006) 014012.
- [35] N. N. Meiman, Sov. Phys. JETP **17** (1963) 830;
B. V. Geshkenbein, B. L. Ioffe, Sov. Phys. JETP **17** (1963) 820;
S. Okubo, Phys. Rev. D **4**, 725 (1971);
C. Bourrely, B. Machet and E. de Rafael, Nucl. Phys. B **189**, 157 (1981).

- [36] C. G. Boyd, B. Grinstein and R. F. Lebed, Phys. Rev. Lett. **74**, 4603 (1995);
L. Lellouch, Nucl. Phys. B **479**, 353 (1996);
M. C. Arnesen, B. Grinstein, I. Z. Rothstein and I. W. Stewart, Phys. Rev. Lett. **95** (2005) 071802.
- [37] T. Becher and R. J. Hill, Phys. Lett. B **633**, 61 (2006).
- [38] S. Descotes-Genon and A. Le Yaouanc, J. Phys. G **35** (2008) 115005.
- [39] M. B. Voloshin, Sov. J. Nucl. Phys. **50** (1989) 105;
C. A. Dominguez, J. G. Korner and K. Schilcher, Phys. Lett. B **248**, 399 (1990).
- [40] P. Ball, JHEP **9901** (1999) 010.